

EDGE-CONTRACTION ON DUAL RIBBON GRAPHS, 2D TQFT, AND THE MIRROR OF ORBIFOLD HURWITZ NUMBERS

OLIVIA DUMITRESCU AND MOTOHICO MULASE

ABSTRACT. We present a new set of axioms for a 2D TQFT formulated on the category of the dual of ribbon graphs with edge-contraction operations as morphisms. Every Frobenius algebra A determines a contravariant functor from this category to the category of elements of the tensor category of Frobenius algebras over A^* . The functor evaluated at connected graphs is the TQFT corresponding to A .

The edge-contraction operations also form an effective tool in various graph enumeration problems, such as counting Grothendieck's dessins d'enfants, simple and double Hurwitz numbers. These counting problems can be solved by the topological recursion, which is the universal mirror B-model corresponding to these counting problems. We show that for the case of orbifold Hurwitz numbers, the mirror objects, the spectral curves and the differential forms on it, are constructed purely from the edge-contraction operations of the counting problem.

CONTENTS

1. Introduction	1
2. Frobenius algebras	6
3. 2D TQFT	8
4. The edge-contraction operations on cell graphs	12
5. The category of cell graphs and the functor Ω_A	18
6. Orbifold Hurwitz numbers as graph enumeration	20
6.1. r -Hurwitz graphs	20
6.2. Construction of Hurwitz graphs for $r = 1$	22
6.3. Construction of r -Hurwitz graphs for $r > 1$	22
6.4. An example	23
6.5. The edge-contraction formulas	24
7. Construction of the mirror spectral curves for orbifold Hurwitz numbers	27
References	30

1. INTRODUCTION

The purpose of the present paper is two-fold: One is to give a new set of axioms for a two-dimensional topological quantum field theory (2D TQFT) formulated on the category of the dual of ribbon graphs. The morphisms of this category are **edge-contraction operations**, which correspond to the degenerations in the moduli space $\overline{\mathcal{M}}_{g,n}$ of stable curves of genus g with n labeled points that create a rational component with 3 special points. The Frobenius algebra structure is naturally encoded in this category of graphs, where edge-contractions represent the multiplication and the comultiplication operations in the algebra.

2010 *Mathematics Subject Classification.* Primary: 14N35, 81T45, 14N10; Secondary: 53D37, 05A15.

Key words and phrases. Topological quantum field theory; topological recursion; Frobenius algebras; ribbon graphs; Hurwitz numbers.

The first author is a member of the Simion Stoilow Institute of Mathematics of the Romanian Academy.

The other purpose of the paper is to identify the mirror B-model objects that enable us to solve certain graph enumeration problems. We consider simple and orbifold Hurwitz numbers in this paper, by giving a graph enumeration formulation for these numbers. We then show that the mirror of these counting problems are constructed from the edge-contraction operations applied to the genus 0 and one-marked point orbifold Hurwitz numbers.

A TQFT of dimension d is a functor Z from the monoidal category of $(d-1)$ -dimensional compact oriented topological manifolds, with d -dimensional oriented cobordism forming morphisms among $(d-1)$ -dimensional boundary manifolds, to the monoidal category of finite-dimensional vector spaces defined over a fixed field K [2, 21]. Since there is only one compact manifold in dimension 1, a 2D TQFT is associated with a unique vector space $A = Z(S^1)$, and the Atiyah-Segal axioms of TQFT makes A a commutative Frobenius algebra. It has been established that 2D TQFTs are classified by finite-dimensional Frobenius algebras [1].

We ask the following question, in the reverse direction:

Question 1.1. *Suppose we are given a finite-dimensional commutative Frobenius algebra. What is the topological or combinatorial realization of the algebra structure that leads to the corresponding 2D TQFT?*

The answer we propose in this paper is the *category of the dual of ribbon graphs*, with edge-contraction operations as morphisms. This category does not carry the information of a specific Frobenius algebra. It represents the structure of algebraic operations in every Frobenius algebra.

A ribbon graph is a graph with the assignment of a cyclic order of incident half-edges at each vertex. The cyclic order induces the ribbon structure to the graph, and it becomes the 1-skeleton of the cell-decomposition of a compact oriented topological surface of genus, say g , by attaching oriented open discs to the graph. Let n be the number of the discs attached. We call this ribbon graph of *type* (g, n) .

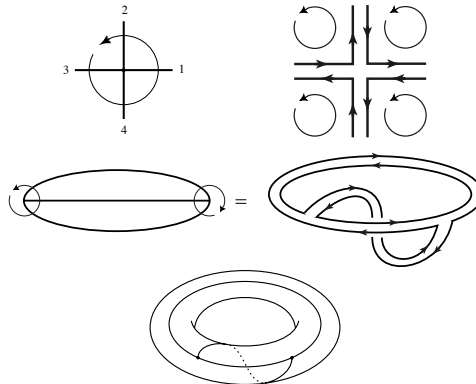


FIGURE 1.1. Top Row: A cyclic order of half-edges at a vertex induces a local ribbon structure to a graph. Second Row: Globally, a ribbon graph becomes the 1-skeleton of a compact oriented surface. Third Row: Thus a ribbon graph is a graph drawn on a compact oriented surface.

An assignment of a positive real number to each edge of a ribbon graph determines a concrete holomorphic coordinate system of the topological surface of genus g with n labeled marked points [17], thus making it a Riemann surface. This construction gives the identification of the space of ribbon graphs of type (g, n) with positive edge lengths assigned,

and the space $\mathcal{M}_{g,n} \times \mathbb{R}_+^n$, as an orbifold. The operation of edge-contraction of an edge connecting two distinct vertices then defines the boundary operator, which introduces on $\mathcal{M}_{g,n} \times \mathbb{R}_+^n$ the structure of orbi-cell complex. Each ribbon graph determines the stratum of this cell complex, whose dimension is the number of edges of the graph.

To emphasize the dual nature, we use the terminology **cell graph** of type (g, n) to indicate the dual of a ribbon graph of the same type. It is also a ribbon graph, and its vertices are labeled. We denote by \mathcal{CG} the category of cell graphs, which are not assumed to be connected. For a pair of cell graphs γ and γ' , the set of morphisms is defined to be $\text{Hom}(\gamma, \gamma') = \text{Aut}(\gamma)$ if $\gamma = \gamma'$, and otherwise, the collection of sequences of edge-contraction operations and graph automorphism that change γ to γ' . This time, we allow any edges to be contracted, including loops.

Let us consider the category \mathcal{F} of finite-dimensional, commutative, Frobenius algebras defined over a fixed field K . For every Frobenius algebra $A \in \text{Ob}(\mathcal{F})$, we denote by \mathcal{F}°/A^* the category of A^* -objects in the dual (opposite) category \mathcal{F}° . Here we note that A and A^* are canonically isomorphic as a vector space, and \mathcal{F}°/A^* is identified as the category of commutative Frobenius A^* -algebras. Define a category $\mathcal{T}(A^*)$ whose objects are the union of all elements in the objects of \mathcal{F}°/A^* . Morphisms are defined by restriction: for $a_k \in M_k \in \text{Ob}(\mathcal{F}^\circ/A^*)$, $k = 1, 2$, we define

$$\text{Hom}(a_1, a_2) := \{\phi \in \text{Hom}(M_1, M_2) \mid \phi(a_1) = a_2\}.$$

Our main result is the following.

Theorem 1.2. *A commutative Frobenius algebra $A \in \text{Ob}(\mathcal{F})$ gives rise to a contravariant functor*

$$(1.1) \quad \Omega_A : \mathcal{CG} \longrightarrow \mathcal{T}(A^*)$$

with the following properties.

- Denote by $\Gamma_{g,n} \subset \text{Ob}(\mathcal{CG})$ the set of connected cell graphs of type (g, n) . Then the image $\Omega_A(\gamma)$ of $\gamma \in \Gamma_{g,n}$ is in $(A^*)^{\otimes n} \in \text{Ob}(\mathcal{F}^\circ/A^*)$.
- $\Omega_A(\gamma)$ is independent of the choice of the graph $\gamma \in \Gamma_{g,n}$, depending only on its type (g, n) . In other words, $\Omega_A(\Gamma_{g,n})$ is a point in $\text{Ob}(\mathcal{T}(A^*))$.
- The assignment $\Gamma_{g,n} \ni \gamma \mapsto \Omega_A(\gamma) \in \{A^{\otimes n} \longrightarrow K\}$ is the 2D TQFT corresponding to the Frobenius algebra A .

The key statement is that the assignment $\gamma \mapsto \Omega_A(\gamma)$ being a functor with respect to edge-contraction operations makes it graph independent within $\Gamma_{g,n}$. This reflects the commutativity, associativity, cocommutativity, and coassociativity of the objects in \mathcal{F} . Our consideration can be generalized to the cohomological field theory of Kontsevich-Manin [16], which will be treated in a forthcoming paper.

The edge-contraction is also an effective method for graph enumeration problems. It has been noted in [10] that the Laplace transform of the edge-contraction operations on many counting problems corresponds to the topological recursion [13]. In this paper, we examine the construction of the mirror B-models corresponding to the simple and orbifold Hurwitz numbers.

In general, enumerative geometry problems, such as computation of Gromov-Witten type invariants, are solved by studying a corresponding problem on the *mirror dual* side. The effectiveness of the mirror problem relies on the technique of complex analysis. The second question we consider in this paper is the following:

Question 1.3. *How do we find the mirror of a given enumerative problem?*

We give an answer to this question for a class of graph enumeration problems that are equivalent to counting of orbifold Hurwitz numbers. The key is again the edge-contraction operation. The base case, or the case for the moduli space $\overline{\mathcal{M}}_{0,1}$, of the edge-contraction in the counting problem identifies the mirror dual object, and a universal mechanism of complex analysis, known as the **topological recursion** of [13], solves the B-model side of the counting problem. The solution is a collection of generating functions of the original problem for all genera.

To illustrate the idea, let us consider the number T_d of connected *trees* consisting of *labeled* d nodes (or vertices). The initial condition is $T_1 = 1$. The numbers satisfy a recursion relation

$$(1.2) \quad (d-1)T_d = \frac{1}{2} \sum_{\substack{a+b=d \\ a,b \geq 1}} ab \binom{d}{a} T_a T_b.$$

A tree of d nodes has $d-1$ edges. The left-hand side counts how many ways we can eliminate an edge. When an edge is eliminated, the tree breaks down into two disjoint pieces, one consisting of a labeled nodes, and the other $b = d - a$ labeled nodes. The original tree is restored by connecting one of the a nodes on one side and one of the b nodes on the other side. The equivalence of counting in this elimination process gives (1.2). From the initial value, the recursion formula generates the tree sequence $1, 1, 3, 16, 125, 1296, \dots$. We note, however, that (1.2) does not directly give a closed formula for T_d . To find one, we introduce a generating function, or a **spectral curve**

$$(1.3) \quad y = y(x) := \sum_{d=1}^{\infty} \frac{T_d}{(d-1)!} x^d.$$

Then (1.2) is equivalent to

$$(1.4) \quad \left(x^2 \circ \frac{d}{dx} \circ \frac{1}{x} \right) y = \frac{1}{2} x \frac{d}{dx} y^2.$$

The initial condition is $y(0) = 0$ and $y'(0) = 1$, which solves the differential equation uniquely as

$$(1.5) \quad x = ye^{-y}.$$

This is a plane analytic curve known as the *Lambert curve*. To find the formula for T_d , we need the *Lagrange Inversion Formula*. Suppose that $f(y)$ is a holomorphic function defined near $y = 0$, and that $f(0) \neq 0$. Then the inverse function of $x = \frac{y}{f(y)}$ near $x = 0$ is given by

$$(1.6) \quad y = \sum_{k=1}^{\infty} \left(\frac{d}{dy} \right)^{k-1} (f(y)^k) \Big|_{y=0} \frac{x^k}{k!}.$$

The proof is elementary and requires only Cauchy's integration formula. Since $f(y) = e^y$ in our case, we immediately obtain Cayley's formula $T_d = d^{d-2}$.

The point we wish to make is that the real problem behind the scene is not tree-counting, but *simple Hurwitz numbers*. This relation is understood by the correspondence between trees and ramified coverings of \mathbb{P}^1 by \mathbb{P}^1 of degree d that are simply ramified except for one total ramification point. When we look at the dual graph of a tree, the edge elimination becomes the edge-contraction operation, and this operation precisely gives a *degeneration formula* for counting problems on $\overline{\mathcal{M}}_{g,n}$. The base case for the counting problem is $(g, n) = (0, 1)$, and the recursion (1.2) is the result of the edge-contraction operation for simple

Hurwitz numbers associated with $\overline{\mathcal{M}}_{0,1}$. Here, the Lambert curve (1.5) is the *mirror dual* of simple Hurwitz numbers.

In the dual picture, T_d counts the number of cell-decompositions of a sphere S^2 consisting of one 0-cell, $(d - 1)$ 1-cells, and d labeled 2-cells. The edge-contraction operation causes the degeneration of \mathbb{P}^1 with one marked point p into two \mathbb{P}^1 's with one marked point on each, connected by a \mathbb{P}^1 with 3 special points, two of which are nodal points and the third one representing the original marked point p . In terms of graph enumeration, the \mathbb{P}^1 with 3 special points does not play any role. So we break the original vertex into two vertices, and separate the graph into two disjoint pieces (Figure 1.2).

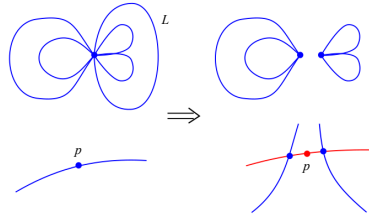


FIGURE 1.2. The edge-contraction operation on a loop is a degeneration process. The graph on the left is a connected cell graph of type $(0, 1)$. The edge-contraction on the loop L changes it to the one on the right. Here, a \mathbb{P}^1 with one marked point p degenerates into two \mathbb{P}^1 's with one marked point on each, connected by a \mathbb{P}^1 with 3 special points.

Bouchard and Mariño [4] conjectured that generating functions for simple Hurwitz numbers could be calculated by the topological recursion of [13], based on the spectral curve (1.5). Here, the notion of spectral curve is the mirror dual object for the counting problem. They arrived at the mirror dual by a consideration of mirror symmetry of toric Calabi-Yau three-folds. The conjecture was solved in a series of papers of one of the authors [12, 19], assuming that the Lambert curve was indeed the mirror. The emphasis of our current paper is that the mirror dual object is simply a consequence of the $\overline{\mathcal{M}}_{0,1}$ case of the edge-contraction operation on the original counting problem. The situation is similar to several cases of Gromov-Witten theory, where the mirror is constructed by the genus 0 Gromov-Witten invariants themselves.

Once we have our formulation of 2D TQFT and topological recursion in terms of edge-contraction operations, we can consider a TQFT-valued topological recursion [7]. An immediate example is the Gromov-Witten theory of the classifying space BG of a finite group G . In [7], we show that a straightforward generalization of the topological recursion for differential forms with values in tensor products of a Frobenius algebra automatically splits into the product of the usual scalar-valued solution to the topological recursion and a 2D TQFT. Therefore, topological recursion implies TQFT. Here, we remark the similarity between the topological recursion and the comultiplication operation in a Frobenius algebra. Indeed, the topological recursion itself can be regarded as a comultiplication formula for an infinite-dimensional analogue of the Frobenius algebra (Vertex algebras, or conformal field theory).

The authors found that the topological recursion appears as the Laplace transform of edge-contraction operations in [10]. The geometric nature of the topological recursion was further investigated in [8, 9], where it was placed in the context of Hitchin spectral curves for the first time, and the relation to quantization was discovered. The present paper

is the authors' first step toward identifying the topological recursion in an algebraic and categorical setting.

The paper is organized as follows. We start with a quick review of Frobenius algebras, for the purpose of setting notations, in Section 2. The category $\mathcal{T}(A)$ is defined. We then recall two-dimensional TQFT in Section 3. In Sections 4 and 5, we give our formulation of 2D TQFT in terms of cell graphs. In Section 6, we present combinatorial graph enumeration problems, and show that they are equivalent to counting of simple and orbifold Hurwitz numbers. Finally in Section 7, the spectral curves of the topological recursion for simple and orbifold Hurwitz numbers (the mirror objects to the counting problems) are constructed from the edge-contraction formulas for $(g, n) = (0, 1)$ invariants.

2. FROBENIUS ALGEBRAS

In the following three sections, we present a new set of axioms for a 2D TQFT. In this paper, we are concerned with a finite-dimensional, unital, and commutative Frobenius algebra A defined over a field K . It has been established in [1] that such an algebra is equivalent to the structure of a 2D TQFT. In this section we set the notation and give the definition of the category $\mathcal{T}(A)$.

Let A be a finite-dimensional, unital, associative, and commutative algebra over a field K . A non-degenerate bilinear form $\eta : A \otimes A \rightarrow K$ is a *Frobenius form* if

$$(2.1) \quad \eta(v_1, m(v_2, v_3)) = \eta(m(v_1, v_2), v_3), \quad v_1, v_2, v_3 \in A,$$

where $m : A \otimes A \rightarrow A$ is the multiplication. We denote by

$$(2.2) \quad \lambda : A \xrightarrow{\sim} A^*, \quad \langle \lambda(u), v \rangle = \eta(u, v),$$

the canonical isomorphism of the algebra A and its dual. We assume that η is a symmetric bilinear form. Let $\mathbf{1} \in A$ denote the multiplicative identity. Then it defines a *counit*, or a *trace*, by

$$(2.3) \quad \epsilon : A \rightarrow K, \quad \epsilon(v) = \eta(\mathbf{1}, v).$$

The canonical isomorphism λ introduces a unique cocommutative and coassociative coalgebra structure in A by the following commutative diagram.

$$(2.4) \quad \begin{array}{ccc} A & \xrightarrow{\delta} & A \otimes A \\ \lambda \downarrow & & \downarrow \lambda \otimes \lambda \\ A^* & \xrightarrow[m^*]{} & A^* \otimes A^* \end{array}$$

It is often convenient to use a basis for calculations. Let $\langle e_1, e_2, \dots, e_r \rangle$ be a K -basis for A . In terms of this basis, the bilinear form η is identified with a symmetric matrix, and its inverse is written as follows:

$$(2.5) \quad \eta = [\eta_{ij}], \quad \eta_{ij} := \eta(e_i, e_j), \quad \eta^{-1} = [\eta^{ij}].$$

The comultiplication is then written as

$$\delta(v) = \sum_{i,j,a,b} \eta(v, m(e_i, e_j)) \eta^{ia} \eta^{jb} e_a \otimes e_b.$$

From now on, if there is no confusion, we denote simply by $m(u, v) = uv$. The symmetric Frobenius form and the commutativity of the multiplication makes

$$(2.6) \quad \eta(e_{i_1} \cdots e_{i_j}, e_{i_{j+1}} \cdots e_n) = \epsilon(e_{i_1} \cdots e_{i_n}), \quad 1 \leq j < n,$$

completely symmetric with respect to permutations of the indices. The following is a standard formula for a non-degenerate bilinear form:

$$(2.7) \quad v = \sum_{a,b} \eta(v, e_a) \eta^{ab} e_b.$$

It immediately follows that

Lemma 2.1. *The following diagram commutes:*

$$(2.8) \quad \begin{array}{ccccc} & & A \otimes A \otimes A & & \\ & \nearrow 1 \otimes \delta & & \searrow m \otimes 1 & \\ A \otimes A & \xrightarrow{m} & A & \xrightarrow{\delta} & A \otimes A \\ & \searrow \delta \otimes 1 & & \nearrow 1 \otimes m & \\ & & A \otimes A \otimes A & & \end{array}$$

Or equivalently, for every v_1, v_2 in A , we have

$$\delta(v_1 v_2) = (1 \otimes m)(\delta(v_1), v_2) = (m \otimes 1)(v_2, \delta(v_1)).$$

Proof. Noticing the commutativity and cocommutativity of A , we have

$$\begin{aligned} \delta(v_1 v_2) &= \sum_{i,j,a,b} \eta(v_1 v_2, e_i e_j) \eta^{ia} \eta^{jb} e_a \otimes e_b \\ &= \sum_{i,j,a,b} \eta(v_1 e_i, v_2 e_j) \eta^{ia} \eta^{jb} e_a \otimes e_b \\ &= \sum_{i,j,a,b,c,d} \eta(v_1 e_i, e_c) \eta^{cd} \eta(e_d, v_2 e_j) \eta^{ia} \eta^{jb} e_a \otimes e_b \\ &= \sum_{i,j,a,b,c,d} \eta(v_1, e_i e_c) \eta^{cd} \eta^{ia} \eta(e_d v_2, e_j) \eta^{jb} e_a \otimes e_b \\ &= \sum_{i,a,c,d} \eta(v_1, e_i e_c) \eta^{cd} \eta^{ia} e_a \otimes (e_d v_2) \\ &= (1 \otimes m)(\delta(v_1), v_2). \end{aligned}$$

□

In the lemma above we consider the composition $\delta \circ m$. The other order of operations plays an essential role in 2D TQFT.

Definition 2.2 (Euler element). The **Euler element** of a Frobenius algebra A is defined by

$$(2.9) \quad \mathbf{e} := m \circ \delta(\mathbf{1}).$$

In terms of basis, the Euler element is given by

$$(2.10) \quad \mathbf{e} = \sum_{a,b} \eta^{ab} e_a e_b.$$

Another application of (2.7) is the following formula that relates the multiplication and comultiplication.

$$(2.11) \quad (\lambda(v_1) \otimes 1) \delta(v_2) = v_1 v_2.$$

This is because

$$\begin{aligned}
(\lambda(v_1) \otimes 1) \delta(v_2) &= \sum_{a,b,k,\ell} (\lambda(v_1) \otimes 1) \eta(v_2, e_k e_\ell) \eta^{ka} \eta^{\ell b} e_a \otimes e_b \\
&= \sum_{a,b,k,\ell} \eta(v_2 e_\ell, e_k) \eta^{ka} \eta(v_1, e_a) \eta^{\ell b} e_b \\
&= \sum_{b,\ell} \eta(v_1, v_2 e_\ell) \eta^{\ell b} e_b = v_1 v_2.
\end{aligned}$$

Let us now consider the category \mathcal{F} of finite-dimensional, commutative, Frobenius algebras. We denote by \mathcal{F}° its dual, or opposite, category. For a Frobenius algebra $A \in \text{Ob}(\mathcal{F})$, the category \mathcal{F}°/A^* consists of Frobenius algebras that are also A^* -algebras.

Definition 2.3 (The category $\mathcal{T}(A^*)$). We define the category $\mathcal{T}(A^*)$ as follows. Let $b_k \in B_k \in \text{Ob}(\mathcal{F}^\circ/A^*)$, $k = 1, 2$.

$$(2.12) \quad \text{Ob}(\mathcal{T}(A^*)) := \coprod_{B \in \text{Ob}(\mathcal{F}^\circ/A^*)} B.$$

$$(2.13) \quad \text{Hom}(b_1, b_2) := \{\phi \in \text{Hom}(B_1, B_2) \mid \phi(b_1) = b_2\}.$$

3. 2D TQFT

The axiomatic formulation of conformal and topological quantum field theories was established in 1980s. We refer to Atiyah [2] and Segal [21]. Here we consider only two-dimensional topological quantum field theories.

A 2D TQFT is a functor Z from the cobordism category of oriented surfaces (a surface being a cobordism of its boundary circles) to the tensor category of finite-dimensional vector spaces over a fixed field K with the operation of tensor products. The Atiyah-Segal TQFT axioms automatically make the vector space

$$(3.1) \quad Z(S^1) = A$$

a unital commutative Frobenius algebra over K .

Let $\Sigma_{g,n}$ be an oriented surface of finite topological type (g, n) , i.e., a surface obtained by removing n disjoint open discs from a compact oriented two-dimensional topological manifold of genus g . The boundary components are labeled by indices $1, \dots, n$. We always give the induced orientation at each boundary circle. The TQFT then assigns to such a surface a multilinear map

$$(3.2) \quad \Omega_{g,n} \stackrel{\text{def}}{=} Z(\Sigma_{g,n}) : A^{\otimes n} \longrightarrow K.$$

If we change the orientation at the i -th boundary, then the i -th factor of the tensor product is changed to the dual space A^* . Therefore, if we have k boundary circles with induced orientation and ℓ circles with opposite orientation, then we have a multi-linear map

$$\Omega_{g,k,\bar{\ell}} : A^{\otimes k} \longrightarrow A^{\otimes \ell}.$$

The sewing axiom of Atiyah [2] requires that

$$\Omega_{g_2, \ell, \bar{n}} \circ \Omega_{g_1, k, \bar{\ell}} = \Omega_{g_1 + g_2 + \ell - 1, k, \bar{n}} : A^{\otimes k} \longrightarrow A^{\otimes n}.$$

A 2D TQFT can be also obtained as a special case of a CohFT of [16].

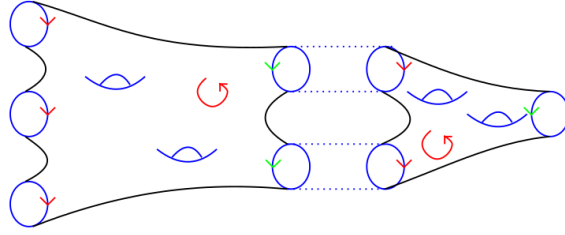


FIGURE 3.1.

Definition 3.1 (Cohomological Field Theory). We denote by $\overline{\mathcal{M}}_{g,n}$ the moduli space of stable curves of genus g and n smooth marked points. Let

$$(3.3) \quad \pi : \overline{\mathcal{M}}_{g,n+1} \longrightarrow \overline{\mathcal{M}}_{g,n}$$

be the forgetful morphism of the last marked point, and

$$(3.4) \quad gl_1 : \overline{\mathcal{M}}_{g-1,n+2} \longrightarrow \overline{\mathcal{M}}_{g,n}$$

$$(3.5) \quad gl_2 : \overline{\mathcal{M}}_{g_1,n_1+1} \times \overline{\mathcal{M}}_{g_2,n_2+1} \longrightarrow \overline{\mathcal{M}}_{g_1+g_2,n_1+n_2}$$

the gluing morphisms that give boundary strata of the moduli space. An assignment

$$(3.6) \quad \Omega_{g,n} : A^{\otimes n} \longrightarrow H^*(\overline{\mathcal{M}}_{g,n}, K)$$

is a CohFT if the following axioms hold:

CohFT 0: $\Omega_{g,n}$ is S_n -invariant, and $\Omega_{0,3}(\mathbf{1}, v_1, v_2) = \eta(v_1, v_2)$.

CohFT 1: $\Omega_{g,n+1}(v_1, \dots, v_n, \mathbf{1}) = \pi^* \Omega_{g,n}(v_1, \dots, v_n)$.

CohFT 2: $gl_1^* \Omega_{g,n}(v_1, \dots, v_n) = \sum_{a,b} \Omega_{g-1,n+2}(v_1, \dots, v_n, e_a, e_b) \eta^{ab}$.

CohFT 3: $gl_2^* \Omega_{g_1+g_2,|I|+|J|}(v_I, v_J) = \sum_{a,b} \Omega_{g_1,|I|+1}(v_I, e_a) \Omega_{g_2,|J|+1}(v_J, e_b) \eta^{ab}$,

where $I \sqcup J = \{1, \dots, n\}$.

If a CohFT takes values in $H^0(\overline{\mathcal{M}}_{g,n}, K) = K$, then it is a 2D TQFT. In what follows, we only consider CohFT with values in $H^0(\overline{\mathcal{M}}_{g,n}, K)$.

Remark 3.2. The forgetful morphism makes sense for a stable pointed curve, but it does not exist for a topological surface with boundary. Certainly we cannot *forget* a boundary. Since $H^0(\overline{\mathcal{M}}_{g,n}, K) = K$ is not affected by the morphism (3.3)-(3.5), the equation

$$\Omega_{g,n}(\mathbf{1}, v_2, \dots, v_n) = \Omega_{g,n-1}(v_2, \dots, v_n)$$

is identified with CohFT 3 for $g_2 = 0$ and $J = \emptyset$ by defining

$$(3.7) \quad \Omega_{0,1}(v) := \epsilon(v) = \eta(\mathbf{1}, v),$$

even though $\overline{\mathcal{M}}_{0,1}$ does not exist. We then have

$$\begin{aligned} \Omega_{g,n}(v_1, \dots, v_n) &= \sum_{a,b} \Omega_{g,n+1}(v_1, \dots, v_n, e_a) \eta(\mathbf{1}, e_b) \eta^{ab} \\ &= \Omega_{g,n+1}(v_1, \dots, v_n, \mathbf{1}) \end{aligned}$$

by (2.7). In other words, the isomorphism of the degree 0 cohomologies

$$(3.8) \quad \pi^* : H^0(\overline{\mathcal{M}}_{g,n}, K) \longrightarrow H^0(\overline{\mathcal{M}}_{g,n+1}, K)$$

is replaced by its left inverse

$$(3.9) \quad \sigma_i^* : H^0(\overline{\mathcal{M}}_{g,n+1}, K) \longrightarrow H^0(\overline{\mathcal{M}}_{g,n}, K),$$

where

$$(3.10) \quad \sigma_i : \overline{\mathcal{M}}_{g,n} \longrightarrow \overline{\mathcal{M}}_{g,n+1}$$

is one of the n tautological sections.

Remark 3.3. In the same spirit, although $\overline{\mathcal{M}}_{0,2}$ does not exist either, we need to *define*

$$(3.11) \quad \Omega_{0,2}(v_1, v_2) := \eta(v_1, v_2)$$

so that we can exhaust all the cases appearing in the Atiyah-Segal axioms for 2D TQFT. In particular, for $g_2 = 0$ and $J = \{n\}$, we have

$$\begin{aligned} \Omega_{g,n}(v_1, \dots, v_n) &= \Omega_{g,n} \left(v_1, \dots, v_{n-1}, \sum_{a,b} \eta(v_n, e_b) \eta^{ab} e_a \right) \\ &= \sum_{a,b} \Omega_{g,n}(v_1, \dots, v_{n-1}, e_a) \Omega_{0,2}(v_n, e_b) \eta^{ab}. \end{aligned}$$

Thus $\Omega_{0,2}(v_1, v_2)$ functions as the identity operator of the Atiyah-Segal axiom [2].

Remark 3.4. A marked point p_i of a stable curve $\Sigma \in \overline{\mathcal{M}}_{g,n}$ is an insertion point for the cotangent class $\psi_i = c_1(\mathbb{L}_i)$, where \mathbb{L}_i is the pull-back of the relative canonical sheaf ω on the universal curve $\pi : \overline{\mathcal{M}}_{g,n+1} \longrightarrow \overline{\mathcal{M}}_{g,n}$ by the i -th tautological section $\sigma_i : \overline{\mathcal{M}}_{g,n} \longrightarrow \overline{\mathcal{M}}_{g,n+1}$. If we cut a small disc around $p_i \in \Sigma$, then the orientation induced on the boundary circle is consistent with the orientation of the unit circle in $T_{p_i}^* \Sigma$. This orientation is opposite to the orientation that is naturally induced on $T_{p_i} \Sigma$. In general, if V is an oriented real vector space of dimension n , then V^* naturally acquires the opposite orientation with respect to the dual basis if $n \equiv 2, 3 \pmod{4}$.

As we have noted, in terms of sewing axioms, if a boundary circle on a topological surface Σ of type (g, n) is oriented according to the induced orientation, then this is an *input* circle to which we assign an element of A . If a boundary circle is oppositely oriented, then it is an *output* circle and Σ produces an output element at this boundary. Thus if Σ_1 has an input circle and Σ_2 an output circle, then we can sew the two surfaces together along the circle to form a connected sum $\Sigma_1 \# \Sigma_2$, where the output from Σ_2 is placed as input for Σ_1 .

Proposition 3.5. *The genus 0 values of a 2D TQFT is given by*

$$(3.12) \quad \Omega_{0,n}(v_1, \dots, v_n) = \epsilon(v_1 \cdots v_n),$$

provided that we define

$$(3.13) \quad \Omega_{0,3}(v_1, v_2, v_3) := \epsilon(v_1 v_2 v_3).$$

Proof. This is a direct consequence of CohFT 3 and (2.7). □

One of the original motivations of TQFT [2, 21] is to identify the *topological invariant* $Z(\Sigma)$ of a closed manifold Σ . In our current setting, it is defined as

$$(3.14) \quad Z(\Sigma_g) := \epsilon(\lambda^{-1}(\Omega_{g,1}))$$

for a closed oriented surface Σ_g of genus g . Here, $\Omega_{g,1} : A \longrightarrow K$ is an element of A^* , and $\lambda : A \xrightarrow{\sim} A^*$ is the canonical isomorphism.

Proposition 3.6. *The topological invariant $Z(\Sigma_g)$ of (3.14) is given by*

$$(3.15) \quad Z(\Sigma_g) = \epsilon(\mathbf{e}^g),$$

where $\mathbf{e}^g \in A$ represents the g -th power of the Euler element of (2.9).

Lemma 3.7. *We have*

$$(3.16) \quad \mathbf{e} := m \circ \delta(1) = \lambda^{-1}(\Omega_{1,1}).$$

Proof. This follows from

$$\Omega_{1,1}(v) = \sum_{a,b} \Omega_{0,3}(v, e_a, e_b) \eta^{ab} = \sum_{a,b} \eta(v, e_a e_b) \eta^{ab} = \eta(v, \mathbf{e})$$

for every $v \in A$. □

Proof of Proposition 3.6. Since the starting case $g = 1$ follows from the above Lemma, we prove the formula by induction, which goes as follows:

$$\begin{aligned} \Omega_{g,1}(v) &= \sum_{a,b} \Omega_{g-1,3}(v, e_a, e_b) \eta^{ab} \\ &= \sum_{i,j,a,b} \Omega_{0,4}(v, e_a, e_b, e_i) \Omega_{g-1,1}(e_j) \eta^{ab} \eta^{ij} \\ &= \sum_{i,j,a,b} \eta(v e_a e_b, e_i) \Omega_{g-1,1}(e_j) \eta^{ab} \eta^{ij} \\ &= \sum_{i,j} \eta(v \mathbf{e}, e_i) \Omega_{g-1,1}(e_j) \eta^{ij} \\ &= \Omega_{g-1,1}(v \mathbf{e}) \\ &= \Omega_{1,1}(v \mathbf{e}^{g-1}) \\ &= \eta(v \mathbf{e}^{g-1}, \mathbf{e}) = \eta(v, \mathbf{e}^g). \end{aligned}$$

□

A closed genus g surface is obtained by sewing g genus 1 pieces with one output boundaries to a genus 0 surface with g input boundaries. Since the Euler element is the output of the genus 1 surface with one boundary, we obtain the same result

$$Z(\Sigma_g) = \Omega_{0,g}(\overbrace{\mathbf{e}, \dots, \mathbf{e}}^g).$$

Finally we have the following:

Theorem 3.8. *The value or the 2D TQFT is given by*

$$(3.17) \quad \Omega_{g,n}(v_1, \dots, v_n) = \epsilon(v_1 \cdots v_n \mathbf{e}^g).$$

Proof. The argument is the same as the proof of Proposition 3.6:

$$\begin{aligned} \Omega_{g,n}(v_1, \dots, v_n) &= \Omega_{1,n}(v_1 \mathbf{e}^{g-1}, v_2, \dots, v_n) \\ &= \sum_{a,b} \Omega_{0,n+2}(v_1 \mathbf{e}^{g-1}, v_2, \dots, v_n, e_a, e_b) \eta^{ab} \\ &= \epsilon(v_1 \cdots v_n \mathbf{e}^g). \end{aligned}$$

□

4. THE EDGE-CONTRACTION OPERATIONS ON CELL GRAPHS

In this section we give a new formulation of a 2D TQFT, based on the edge-contraction operations on cell graphs and a different set of axioms.

Definition 4.1 (Cell graphs). A connected **cell graph** of topological type (g, n) is the 1-skeleton of a cell-decomposition of a connected compact oriented topological surface of genus g with n labeled 0-cells. We call a 0-cell a *vertex*, a 1-cell an *edge*, and a 2-cell a *face*, of a cell graph.

Remark 4.2. The *dual* of a cell graph is usually referred to as a *ribbon graph*, or a *dessin d'enfant* of Grothendieck. A ribbon graph is a graph with cyclic order assigned to incident half-edges at each vertex. Such assignments induce a cyclic order on half-edges at each vertex of the dual graph. Thus a cell graph itself is a ribbon graph. We note that vertices of a cell graph are labeled, which corresponds to the usual face labeling of a ribbon graph.

Remark 4.3. We identify two cell graphs if there is a homeomorphism of the surfaces that brings one cell-decomposition to the other, keeping the labeling of 0-cells. The only possible automorphisms of a cell graph come from cyclic rotations of half-edges at each vertex. If we place an outgoing arrow to one of the half-edges incident to every vertex [10, 18], then there is no automorphism any more. Such a cell graph is called an **arrowed cell graph**.

We denote by $\Gamma_{g,n}$ the set of connected cell graphs of type (g, n) with labeled vertices.

Definition 4.4 (Edge-contraction axioms). The **edge-contraction axioms** are the following set of rules for the assignment

$$(4.1) \quad \Omega : \Gamma_{g,n} \longrightarrow (A^*)^{\otimes n}$$

of a multilinear map

$$\Omega(\gamma) : A^{\otimes n} \longrightarrow K$$

to each cell graph $\gamma \in \Gamma_{g,n}$. We consider $\Omega(\gamma)$ an n -variable function $\Omega(\gamma)(v_1, \dots, v_n)$, where we assign $v_i \in A$ to the i -th vertex of γ .

- **ECA 0:** For the simplest cell graph $\gamma_0 \in \Gamma_{0,1}$ that consists of only one vertex without any edges, we define

$$(4.2) \quad \Omega(\gamma_0)(v) = \epsilon(v), \quad v \in A.$$

- **ECA 1:** Suppose there is an edge E connecting the i -th vertex and the j -th vertex for $i < j$ in $\gamma \in \Gamma_{g,n}$. Let $\gamma' \in \Gamma_{g,n-1}$ denote the cell graph obtained by contracting E . Then

$$(4.3) \quad \Omega(\gamma)(v_1, \dots, v_n) = \Omega(\gamma')(v_1, \dots, v_{i-1}, v_i v_j, v_{i+1}, \dots, \widehat{v_j}, \dots, v_n),$$

where $\widehat{v_j}$ means we omit the j -th variable v_j at the j -th vertex, which no longer exists in γ' .

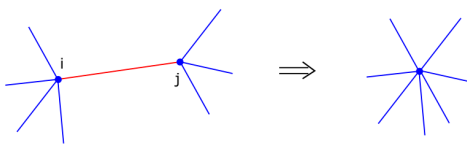


FIGURE 4.1.

- **ECA 2:** Suppose there is a loop L in $\gamma \in \Gamma_{g,n}$ at the i -th vertex. Let γ' denote the possibly disconnected graph obtained by contracting L and separating the vertex to two distinct vertices labeled by i and i' . For the purpose of labeling all vertices, we assign an ordering $i-1 < i < i' < i+1$.

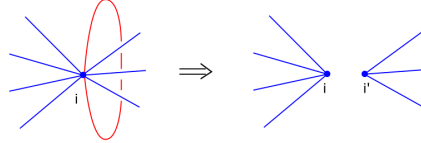


FIGURE 4.2.

If γ' is connected, then it is in $\Gamma_{g-1,n+1}$. We call L a *loop of a handle*. We then impose

$$(4.4) \quad \Omega(\gamma)(v_1, \dots, v_n) = \Omega(\gamma')(v_1, \dots, v_{i-1}, \delta(v_i), v_{i+1}, \dots, v_n),$$

where the outcome of the comultiplication $\delta(v_i)$ is placed in the i -th and i' -th slots.

If γ' is disconnected, then write $\gamma' = (\gamma_1, \gamma_2) \in \Gamma_{g_1, |I|+1} \times \Gamma_{g_2, |J|+1}$, where

$$(4.5) \quad \begin{cases} g = g_1 + g_2 \\ I \sqcup J = \{1, \dots, \hat{i}, \dots, n\} \end{cases}.$$

In this case L is a *separating loop*. Here, vertices labeled by I belong to the connected component of genus g_1 , and those labeled by J on the other component. Let (I_-, i, I_+) (reps. (J_-, i, J_+)) be reordering of $I \sqcup \{i\}$ (resp. $J \sqcup \{i\}$) in the increasing order. We impose

$$(4.6) \quad \Omega(\gamma)(v_1, \dots, v_n) = \sum_{a,b,k,\ell} \eta(v_i, e_k e_\ell) \eta^{ka} \eta^{\ell b} \Omega(\gamma_1)(v_{I_-}, e_a, v_{I_+}) \Omega(\gamma_2)(v_{J_-}, e_b, v_{J_+}),$$

which is similar to (4.4), just the comultiplication $\delta(v_i)$ is written in terms of the basis. Here, cocommutativity of A is assumed in this formula.

Remark 4.5. We do not assume the permutation symmetry of $\Omega(\gamma)(v_1, \dots, v_n)$. The cumbersome notation of the axioms is due to keeping track of the ordering of indices.

Remark 4.6. Let us define $m(\gamma) = 2g - 2 + n$ for $\gamma \in \Gamma_{g,n}$. The edge-contraction operations are reduction of $m(\gamma)$ exactly by 1. Indeed, for ECA 1, we have

$$m(\gamma') = 2g - 2 + (n - 1) = m(\gamma) - 1.$$

The ECA 2 applied to a loop of a handle produces

$$m(\gamma') = 2(g - 1) - 2 + (n + 1) = m(\gamma) - 1.$$

For a separating loop, we have

$$+ \frac{2g_1 - 2 + |I| + 1}{2g_2 - 2 + |J| + 1} = 2g - 2 + n - 1.$$

This reduction is used in the proof of the following theorem.

Theorem 4.7 (Graph independence). *As the consequence of the edge-contraction axioms, every connected cell graph $\gamma \in \Gamma_{g,n}$ gives rise to the same map*

$$(4.7) \quad \Omega(\gamma) : A^{\otimes n} \ni v_1 \otimes \cdots \otimes v_n \mapsto \epsilon(v_1 \cdots v_n \mathbf{e}^g) \in K,$$

where \mathbf{e} is the Euler element of (2.9). In particular, $\Omega(\gamma)(v_1, \dots, v_n)$ is symmetric with respect to permutation of indices.

Corollary 4.8 (ECA implies TQFT). *Define $\Omega_{g,n}(v_1, \dots, v_n) = \Omega(\gamma)(v_1, \dots, v_n)$ for any $\gamma \in \Gamma_{g,n}$. Then $\{\Omega_{g,n}\}$ is the 2D TQFT associated with the Frobenius algebra A . Every 2D TQFT is obtained in this way, hence the two descriptions of 2D TQFT are equivalent.*

Proof of Corollary 4.8 assuming Theorem 4.7. Since both ECAs and 2D TQFT give the unique value

$$\Omega(\gamma)(v_1, \dots, v_n) = \epsilon(v_1 \cdots v_n \mathbf{e}^g) = \Omega_{g,n}(v_1, \dots, v_n)$$

for all (g, n) from (3.17), we see that the two sets of axioms are equivalent, and also that the edge-contraction axioms produce all 2D TQFTs. \square

To illustrate the graph independence, let us first examine three simple cases.

Lemma 4.9 (Edge-removal lemma). *Let $\gamma \in \Gamma_{g,n}$.*

- (1) *Suppose there is a disc-bounding loop L in γ (the graph on the left of Figure 4.3). Let $\gamma' \in \Gamma_{g,n}$ be the graph obtained by removing L from γ .*
- (2) *Suppose there are two edges E_1 and E_2 between two distinct vertices Vertex i and Vertex j , $i < j$, that bound a disc (the middle graph of Figure 4.3). Let $\gamma' \in \Gamma_{g,n}$ be the graph obtained by removing E_2 .*
- (3) *Suppose two loops, L_1 and L_2 , are attached to the i -th vertex (the graph on the right of Figure 4.3). If they are homotopic, then let $\gamma' \in \Gamma_{g,n}$ be the graph obtained by removing L_2 from γ .*

In each of the above cases, we have

$$(4.8) \quad \Omega(\gamma)(v_1, \dots, v_n) = \Omega(\gamma')(v_1, \dots, v_n).$$

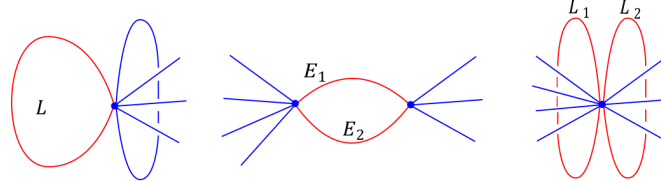


FIGURE 4.3.

Proof. (1) Contracting a disc-bounding loop attached to the i -th vertex creates $(\gamma_0, \gamma') \in \Gamma_{0,1} \times \Gamma_{g,n}$, where γ_0 consists of only one vertex and no edges. Then ECA 2 reads

$$\begin{aligned} \Omega(\gamma)(v_1, \dots, v_n) &= \sum_{a,b,k,\ell} \eta(v_i, e_k e_\ell) \eta^{ka} \eta^{\ell b} \gamma_0(e_a) \Omega(\gamma')(v_1, \dots, v_{i-1}, e_b, v_{i+1}, \dots, v_n) \\ &= \sum_{a,b,k,\ell} \eta(v_i, e_k e_\ell) \eta^{ka} \eta^{\ell b} \eta(1, e_a) \Omega(\gamma')(v_1, \dots, v_{i-1}, e_b, v_{i+1}, \dots, v_n) \\ &= \sum_{b,k,\ell} \eta(v_i, e_k e_\ell) \delta_1^k \eta^{\ell b} \Omega(\gamma')(v_1, \dots, v_{i-1}, e_b, v_{i+1}, \dots, v_n) \end{aligned}$$

$$\begin{aligned}
&= \sum_{b,\ell} \eta(v_i, e_\ell) \eta^{\ell b} \Omega(\gamma')(v_1, \dots, v_{i-1}, e_b, v_{i+1}, \dots, v_n) \\
&= \Omega(\gamma')(v_1, \dots, v_{i-1}, v_i, v_{i+1}, \dots, v_n).
\end{aligned}$$

(2) Contracting Edge E_1 makes E_2 a disc-bounding loop at Vertex i . We can remove it by (1). Note that the new Vertex i is assigned with $v_i v_j$. Restoring E_1 makes the graph exactly the one obtained by removing Edge E_2 from γ . Thus (4.8) holds.

(3) Contracting Loop L_1 makes L_2 a disc-bounding loop. Hence we can remove it by (1). Then restoring L_1 creates a graph obtained from γ by removing L_2 . Thus (4.8) holds. \square

Remark 4.10. The three cases treated above correspond to eliminating degree 1 and 2 vertices from the dual ribbon graph.

Definition 4.11 (Reduced graph). We call a cell graph **reduced** if it does not have any disc-bounding loops or disc-bounding bigons. In other words, the dual ribbon graph of a reduced cell graph has no vertices of degree 1 or 2.

We can see from Lemma 4.9 (1) that every $\gamma_{0,1} \in \Gamma_{0,1}$ gives rise to the same map

$$(4.9) \quad \Omega(\gamma_{0,1})(v) = \epsilon(v).$$

Likewise, Lemma 4.9 (1) and (2) show that every $\gamma_{0,2} \in \Gamma_{0,2}$ gives the same map

$$\Omega(\gamma_{0,2})(v_1, v_2) = \eta(v_1, v_2).$$

This is because we can remove all edges and loops but one that connects the two vertices, and from ECA 1, the value of the assignment is $\epsilon(v_1 v_2)$.

Proof of Theorem 4.7. We use the induction on $m = 2g - 2 + n$. The base case is $m = -1$, or $(g, n) = (0, 1)$, for which the theorem holds by (4.9). Assume that (4.7) holds for all (g, n) with $2g - 2 + n < m$. Now let $\gamma \in \Gamma_{g,n}$ be a cell graph of type (g, n) such that $2n - 2 + n = m$.

Choose an arbitrary straight edge of γ that connects two distinct vertices, say Vertex i and Vertex j , $i < j$. By contracting this edge, we obtain by ECA 1,

$$\Omega(\gamma)(v_1, \dots, v_n) = \Omega(\gamma_{g,n-1})(v_1, \dots, v_{i-1}, v_i v_j, v_{i+1}, \dots, \hat{v}_j, \dots, v_n) = \epsilon(v_1 \dots v_n \mathbf{e}^g).$$

If we have chosen an arbitrary loop attached to Vertex i , then its contraction by ECA 2 gives two cases, depending on whether the loop is a loop of a handle, or a separating loop. For the first case, by appealing to (2.7) and (2.10), we obtain

$$\begin{aligned}
\Omega(\gamma)(v_1, \dots, v_n) &= \sum_{a,b,k,\ell} \eta(v_i, e_k e_\ell) \eta^{ka} \eta^{\ell b} \Omega(\gamma_{g-1,n+1})(v_1, \dots, v_{i-1}, e_a, e_b, v_{i+1}, \dots, v_n) \\
&= \sum_{a,b,k,\ell} \eta(v_i e_k, e_\ell) \eta^{ka} \eta^{\ell b} \Omega(\gamma_{g-1,n+1})(v_1, \dots, v_{i-1}, e_a, e_b, v_{i+1}, \dots, v_n) \\
&= \sum_{a,k} \eta^{ka} \Omega(\gamma_{g-1,n+1})(v_1, \dots, v_{i-1}, e_a, v_i e_k, v_{i+1}, \dots, v_n) \\
&= \sum_{a,k} \eta^{ka} \epsilon(v_1 \dots v_n \mathbf{e}^{g-1} e_a e_b) \\
&= \epsilon(v_1 \dots v_n \mathbf{e}^g).
\end{aligned}$$

For the case of a separating loop, again by appealing to (2.7), we have

$$\Omega(\gamma)(v_1, \dots, v_n) = \sum_{a,b,k,\ell} \eta(v_i, e_k e_\ell) \eta^{ka} \eta^{\ell b} \Omega(\gamma_{g_1,|I|+1})(v_{I-}, e_a, v_{I+}) \Omega(\gamma_{g_2,|J|+1})(v_{J-}, e_b, v_{J+})$$

$$\begin{aligned}
&= \sum_{a,b,k,\ell} \eta(v_i, e_k e_\ell) \eta^{ka} \eta^{\ell b} \epsilon \left(e_a \prod_{c \in I} v_c \mathbf{e}^{g_1} \right) \epsilon \left(e_b \prod_{d \in J} v_d \mathbf{e}^{g_2} \right) \\
&= \sum_{a,b,k,\ell} \eta(v_i e_k, e_\ell) \eta^{ka} \eta^{\ell b} \eta \left(\prod_{c \in I} v_c, e_a \mathbf{e}^{g_1} \right) \epsilon \left(e_b \prod_{d \in J} v_d \mathbf{e}^{g_2} \right) \\
&= \sum_{a,k} \eta^{ka} \eta \left(\prod_{c \in I} v_c \mathbf{e}^{g_1}, e_a \right) \epsilon \left(v_i e_k \prod_{d \in J} v_d \mathbf{e}^{g_2} \right) \\
&= \epsilon \left(v_i \prod_{c \in I} v_c \mathbf{e}^{g_1} \prod_{d \in J} v_d \mathbf{e}^{g_2} \right) \\
&= \epsilon(v_1 \cdots v_n \mathbf{e}^{g_1+g_2}).
\end{aligned}$$

Therefore, no matter how we apply ECA 1 or ECA 2, we always obtain the same result. This completes the proof. \square

The main reason for the graph independence, Theorem 4.7, is the property of the Frobenius algebra A that we have, namely, commutativity, cocommutativity, associativity, coassociativity, and the Frobenius relation (2.1). These properties are manifest in the following graph operations. Although the next proposition is an easy consequence of Theorem 4.7, we derive it directly from the ECAs so that we can see how the algebraic structure of the Frobenius algebra is encoded into the TQFT. Indeed, the graph-independence theorem also follows from Proposition 4.12.

Proposition 4.12 (Commutativity of Edge Contractions). *Let $\gamma \in \Gamma_{g,n}$.*

(1) *Suppose Vertex i is connected to two distinct vertices Vertex j and Vertex k by two edges, E_j and E_k . The graph we obtain, denoted as $\gamma' \in \Gamma_{g,n-2}$, by first contracting E_j and then contracting E_k , is the same as contracting the edges in the opposite order. The two different orders of the application of ECA 1 then gives the same answer. For example, if $i < j < k$, then we have*

$$(4.10) \quad \Omega(\gamma)(v_1, \dots, v_n) = \Omega(\gamma')(v_1, \dots, v_{i-1}, v_i v_j v_k, v_{i+1}, \dots, \hat{v}_j, \dots, \hat{v}_k, \dots, v_n).$$

(2) *Suppose two loops L_1 and L_2 are connected to Vertex i . Then the contraction of the two loops in different orders gives the same result.*

(3) *Suppose a loop L and a straight edge E are attached to Vertex i , where E connects to Vertex j , $i \neq j$. Then contracting L first and followed by contracting E , gives the same result as we contract L and E in the other way around.*

Proof. (1) There are three possible cases: $i < j < k$, $j < i < k$, and $j < k < i$. In each case, the result is replacing v_i by $v_i v_j v_k$, and remove two vertices. The associativity and commutativity of the multiplication of A make the result of different contractions the same.

(2) There are two cases here: After the contraction of one of the loops, (a) the other loop remains to be a loop, or (b) becomes an edge connecting the two vertices created by the contraction of the first loop.

In the first case (a), the contraction of the two loops makes Vertex i in γ into three different vertices i_1, i_2, i_3 of the resulting graph γ' , which may be disconnected. The loop contractions in the two different orders produce triple tensor products

$$(1 \otimes \delta)\delta(v_i) = (\delta \otimes 1)\delta(v_i),$$

which are equal by the coassociativity

$$\begin{array}{ccccc}
 & & A \otimes A & & \\
 & \delta \nearrow & & \searrow 1 \otimes \delta & \\
 A & & & & A \otimes A \otimes A \\
 & \searrow \delta & & \nearrow \delta \otimes 1 & \\
 & & A \otimes A & &
 \end{array}$$

For (b), the contraction of the loops in either order will produce $m \circ \delta(v_i)$ on the same i -th slot of the same graph $\gamma' \in \Gamma_{g-1,n}$.

(3) This amounts to proving the equation

$$\delta(v_i v_j) = (1 \otimes m)(\delta(v_i), v_j) = (m \otimes 1)(v_j, \delta(v_i)),$$

which is Lemma 2.1. \square

Remark 4.13. If we have a system of subsets $\Gamma'_{g,n} \subset \Gamma_{g,n}$ for all (g,n) that is closed under the edge-contraction operations, then all statements of this section still hold by replacing $\Gamma_{g,n}$ by $\Gamma'_{g,n}$.

Remark 4.14. Chen [5] proved the graph independence for a special case of $A = Z\mathbb{C}[S_3]$, the center of the group algebra for symmetric group S_3 , by direct computation. This result led the authors to find a general proof of Theorem 4.7.

The edge-contraction operations are associated with gluing morphisms of $\overline{\mathcal{M}}_{g,n}$ that are different from those in (3.4) and (3.5). ECA 1 of (4.3) is associated with

$$(4.11) \quad \alpha : \overline{\mathcal{M}}_{0,3} \times \overline{\mathcal{M}}_{g,n-1} \longrightarrow \overline{\mathcal{M}}_{g,n}.$$

The handle cutting case of ECA 2 of (4.4) is associated with

$$(4.12) \quad \beta_1 : \overline{\mathcal{M}}_{0,3} \times \overline{\mathcal{M}}_{g-1,n+1} \longrightarrow \overline{\mathcal{M}}_{g,n},$$

and the separating loop contraction with

$$(4.13) \quad \beta_2 : \overline{\mathcal{M}}_{0,3} \times \overline{\mathcal{M}}_{g_1,|I|+1} \times \overline{\mathcal{M}}_{g_2,|J|+1} \longrightarrow \overline{\mathcal{M}}_{g_1+g_2,|I|+|J|+1}.$$

Although there are no cell graph operations that are directly associated with the forgetful morphism π and the gluing maps gl_1 and gl_2 , there is an operation on cell graphs similar to the *connected sum* of topological surfaces.

Definition 4.15 (Connected sum of cell graphs). Let γ' be a cell graph with the following conditions.

- (1) There is a vertex q in γ' of degree d .
- (2) There are d distinct edges incident to q . In particular, none of them is a loop.
- (3) There are exactly d faces in γ' incident to q .

Given an arbitrary cell graph γ with a degree d vertex p , we can create a new cell graph $\gamma \#_{(p,q)} \gamma'$, which we call the *connected sum* of γ and γ' . The procedure is the following. We label all half-edges incident to p with $\{1, 2, \dots, d\}$ according to the cyclic order of the cell graph γ at p . We also label all edges incident to q in γ' with $\{1, 2, \dots, d\}$, but this time opposite to the cyclic order given to γ' at q . Cut a small disc around p and q , and connect all half-edges according to the labeling. The result is a cell graph $\gamma \#_{(p,q)} \gamma'$.

Remark 4.16. The connected sum construction can be applied to two distinct vertices p and q of the same graph, provided that these vertices satisfy the required conditions.

Remark 4.17. The total number of vertices decreases by 2 in the connected sum. Therefore, two 1-vertex graphs cannot be connected by this construction.

The connected sum construction provides the inverse of the edge-contraction operations as the following diagrams show. It is also clear from these figures that the edge-contraction operations are degeneration of curves producing a rational curve with three special points, as indicated in Introduction.

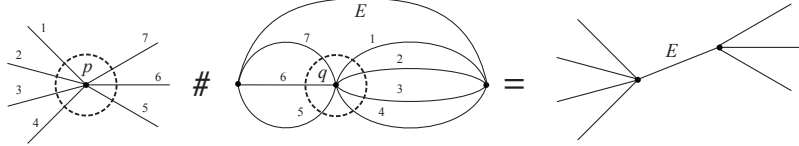


FIGURE 4.4. The connected sum of a cell graph with a particular type $(0, 3)$ cell graph gives the inverse of the edge-contraction operation on E that connects two distinct vertices. The connected sum with the $(0, 3)$ piece has to be done so that the edges incident on each side of E match the original graph.

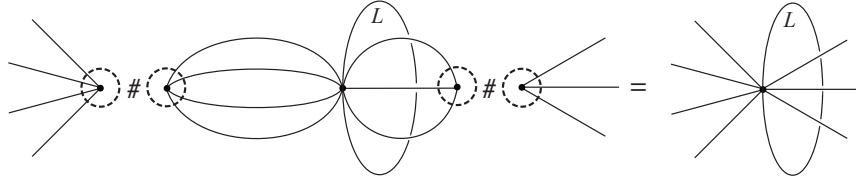


FIGURE 4.5. The edge-contraction operation on a loop L is the inverse of two connected sum operations, with a type $(0, 3)$ piece in the middle.

5. THE CATEGORY OF CELL GRAPHS AND THE FUNCTOR Ω_A

As we have seen in the previous section, the edge-contraction operation is a process of degeneration of a smooth curve in $\mathcal{M}_{g,n}$ that creates a component of a rational curve with 3 special points. If we imagine evolution as the opposite of degeneration, then a cell graph can be considered as a history of evolution of a Riemann surface on which it is drawn. A 2D TQFT depends only on the final outcome, not on the history of evolution. Thus for the purpose of formulating a 2D TQFT on the category of cell graphs, we need to consider edge-contraction operations as morphisms between cell graphs. For this purpose, we give the following definition.

Definition 5.1 (Edge-contraction transformation). An edge-contraction transformation is the composition of a series of edge-contraction operations that are described in Definition 4.4, and cell graph automorphisms, in any order.

For a cell graph $\gamma \in \Gamma_{g,n}$ and $\gamma' \in \Gamma_{g,n-1}$ that is obtained by contracting an edge E , let $a \in \text{Aut}(\gamma)$ and $b \in \text{Aut}(\gamma')$. We denote by ec_E the contraction operation of E on γ . Then $b \circ ec_E \circ a$ is an example of edge-contraction transformations.

Definition 5.2 (The category of cell graphs). The category \mathcal{CG} of cell graphs is defined as follows. First, we consider cell graphs to be not necessarily connected, but their vertices are totally ordered.

$$(5.1) \quad \text{Ob}(\mathcal{CG}) := \text{the set of cell graphs with totally ordered vertices.}$$

For two objects γ and γ' , we define

$$(5.2) \quad \text{Hom}(\gamma, \gamma') := \text{the set of edge-contraction transformations that brings } \gamma \text{ to } \gamma'.$$

In particular, $\text{Hom}(\gamma, \gamma) = \text{Aut}(\gamma)$. If there is no edge-contraction operation that changes γ to γ' , then $\text{Hom}(\gamma, \gamma')$ is the empty set.

Theorem 5.3 (Functor Ω_A). *Given a finite-dimensional commutative Frobenius algebra $A \in \text{Ob}(\mathcal{F})$, the assignment*

$$(5.3) \quad \Omega_A : \text{Ob}(\mathcal{CG}) \ni \gamma \longmapsto \Omega(\gamma) \in (A^*)^{\otimes n} \subset \text{Ob}(\mathcal{T}(A^*))$$

of Definition 4.4 determines a contravariant functor

$$\Omega_A : \mathcal{CG} \longrightarrow \mathcal{T}(A^*).$$

For a disjoint union $\gamma = \gamma_1 \sqcup \gamma_2$, the functor assigns

$$(5.4) \quad \Omega_A(\gamma_1 \sqcup \gamma_2) := \Omega_A(\gamma_1) \otimes \Omega_A(\gamma_2).$$

Proof. We need to show that the morphisms are mapped accordingly. Suppose γ and γ' are as in (4.3), and the edge E of γ , which is an element of $\text{Hom}(\gamma, \gamma')$, connects Vertex i and Vertex j with $i < j$. Let us denote by

$$m_{ij}^* : (A^*)^{\otimes(n-1)} \longrightarrow (A^*)^{\otimes n}$$

the dual of the multiplication m in A operated at the i -th factor of $(A^*)^{\otimes(n-1)}$, and put the result in $(A^*)^{\otimes n}$ at the i -th and j -th positions. The operation is the identity for all other factors. The edge-contraction axiom (4.3) states that $m_{ij}^*(\gamma') = \gamma$, hence

$$m_{ij}^* = \Omega_A(E) \in \text{Hom}(\gamma', \gamma).$$

If we have γ and γ' in the situation of (4.4), then the loop L at Vertex i is in $\text{Hom}(\gamma, \gamma')$. Let

$$\delta_i^* : (A^*)^{\otimes(n+1)} \longrightarrow (A^*)^{\otimes n}$$

be the dual of the comultiplication in A that is operated at the i -th and the next slots of $(A^*)^{\otimes(n+1)}$. By (4.4), we have

$$\delta_i^* = \Omega_A(L) \in \text{Hom}(\gamma', \gamma).$$

Finally, suppose γ, γ_1 , and γ_2 are as in (4.6). This time, let

$$\delta_i^* : (A^*)^{\otimes(|I|+1)} \otimes (A^*)^{\otimes(|J|+1)} \longrightarrow (A^*)^{\otimes n}$$

be operated at the i -th slot of each factor as indicated in (4.6). Then

$$\delta_i^* = \Omega_A(L) \in \text{Hom}(\gamma_1 \sqcup \gamma_2, \gamma).$$

Note that the functor sends $\text{Aut}(\gamma)$ to the trivial morphism in $\mathcal{T}(A^*)$. Since all morphisms in \mathcal{CG} are generated by the above atomic morphisms, we have established that

$$\Omega_A : \text{Hom}(\gamma, \gamma') \longrightarrow \text{Hom}(\Omega_A(\gamma'), \Omega_A(\gamma)).$$

This completes the proof. \square

The results from the previous section then complete the proof of Theorem 1.2.

6. ORBIFOLD HURWITZ NUMBERS AS GRAPH ENUMERATION

Mirror symmetry provides an effective tool for counting problems of Gromov-Witten type invariants. The question is how we construct the mirror, given a counting problem. Although there is so far no general formalism, we present a systematic procedure for computing orbifold Hurwitz numbers in this second part of the paper. The key observation is that the edge-contraction operations for $(g, n) = (0, 1)$ identify the mirror object.

The topological recursion for simple and orbifold Hurwitz numbers are derived as the Laplace transform of the cut-and-join equation [3, 12, 19], where the spectral curves are identified by the consideration of mirror symmetry of toric Calabi-Yau orbifolds [3, 4]. In this section we give a purely combinatorial graph enumeration problem that is equivalent to counting orbifold Hurwitz numbers. We then show in the next section that the edge-contraction formula restricted to the $(g, n) = (0, 1)$ case determines the spectral curve and the differential forms $W_{0,1}$ and $W_{0,2}$ of [3]. These quantities are the mirror objects for the orbifold Hurwitz numbers.

6.1. r -Hurwitz graphs. We choose and fix a positive integer r . The decorated graphs we wish to enumerate are the following.

Definition 6.1 (r -Hurwitz graph). An r -**Hurwitz graph** (γ, D) of type (g, n, d) consists of the following data.

- γ is a connected cell graph of type (g, n) , with n labeled vertices as in earlier sections.
- $|D| = d$ is divisible by r , and γ has $m = d/r$ unlabeled faces and s unlabeled edges, where

$$(6.1) \quad s = 2g - 2 + \frac{d}{r} + n.$$

- D is a configuration of $d = rm$ unlabeled dots on the graph subject to the following conditions:
 - (1) The set of d dots are grouped into m subsets of r dots, each of which is equipped with a cyclic order.
 - (2) Every face of γ has cyclically ordered r dots.
 - (3) These dots are clustered near vertices of the face. At each corner of the face, say at Vertex i , the dots are ordered according to the cyclic order that is consistent of the orientation of the face, which is chosen to be counter-clock wise.
 - (4) Let μ_i denote the total number of dots clustered at Vertex i . Then $\mu_i > 0$ for every $i = 1, \dots, n$. Thus we have an ordered partition

$$(6.2) \quad d = \mu_1 + \dots + \mu_n.$$

In particular, the number of vertices ranges $0 < n \leq d$.

- (5) Suppose an edge E connecting two distinct vertices, say Vertex i and j , bounds the same face twice. Let p be the midpoint of E . The polygon representing the face has E twice on its perimeter, hence the point p appears also twice. We name them as p and p' . Which one we call p or p' does not matter. Consider a path on the perimeter of this polygon starting from p and ending up with p' according to the counter-clock wise orientation. Let r' be the total number of dots clustered around vertices of the face, counted along the path. Then it satisfies

$$(6.3) \quad 0 < r' < r.$$

For example, not all r dots of a face can be clustered at a vertex of degree 1. In particular, for the case of $r = 1$, the graph γ has no edges bounding the same face twice.

An **arrowed** r -Hurwitz graph (γ, \vec{D}) has, in addition to the above data (γ, D) , an arrow assigned to one of the μ_i dots from Vertex i for each index $1 \leq i \leq n$.

The counting problem we wish to study is the number $\mathcal{H}_{g,n}^r(\mu_1, \dots, \mu_n)$ of arrowed r -Hurwitz graphs for a prescribed ordered partition (6.2), counted with the automorphism weight. The combinatorial data corresponds to an object in algebraic geometry. Let us first identify what the r -Hurwitz graphs represent. We denote by $\mathbb{P}^1[r]$ the 1-dimensional orbifold modeled on \mathbb{P}^1 that has one stacky point $[0/(\mathbb{Z}/(r))]$ at $0 \in \mathbb{P}^1$.

Example 6.1. The base case is $\mathcal{H}_{0,1}^r(r) = 1$ (see Figure 6.1). This counts the identity morphism $\mathbb{P}^1[r] \xrightarrow{\sim} \mathbb{P}^1[r]$.

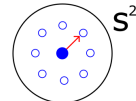


FIGURE 6.1. The graph has only one vertex and no edges. All r dots are clustered around this unique vertex, with an arrow attached to one of them. Because of the arrow, there is no automorphism of this graph.

Definition 6.2 (Orbifold Hurwitz cover and Orbifold Hurwitz numbers). An *orbifold Hurwitz cover* $f : C \rightarrow \mathbb{P}^1[r]$ is a morphism from an orbifold C that is modeled on a smooth algebraic curve of genus g that has

- (1) m stacky points of the same type as the one on the base curve that are all mapped to $[0/(\mathbb{Z}/(r))] \in \mathbb{P}^1[r]$,
- (2) arbitrary profile (μ_1, \dots, μ_n) with n labeled points over $\infty \in \mathbb{P}^1[r]$,
- (3) and all other ramification points are simple.

If we replace the target orbifold by \mathbb{P}^1 , then the morphism is a regular map from a smooth curve of genus g with profile $(\overbrace{r, \dots, r}^m)$ over $0 \in \mathbb{P}^1$, labeled profile (μ_1, \dots, μ_n) over $\infty \in \mathbb{P}^1$, and a simple ramification at any other ramification point. The Euler characteristic condition (6.1) of the graph γ gives the number of simple ramification points of f through the Riemann-Hurwitz formula. The automorphism weighted count of the number of the topological types of such covers is denoted by $H_{g,n}^r(\mu_1, \dots, \mu_n)$. These numbers are referred to as *orbifold Hurwitz numbers*. When $r = 1$, they count the usual simple Hurwitz numbers.

The counting of the topological types is the same as counting actual orbifold Hurwitz covers such that all simple ramification points are mapped to one of the s -th roots of unity ξ^1, \dots, ξ^s , where $\xi = \exp(2\pi i/s)$, if all simple ramification points of f are labeled. Indeed, such a labeling is given by elements of the cyclic group $\{\xi^1, \dots, \xi^s\}$ of order s . Let us construct an edge-labeled Hurwitz graph from an orbifold Hurwitz cover with fixed branch points on the target as above. We first review the case of $r = 1$, i.e., the simple Hurwitz covers. Our graph is essentially the same as the dual of the *branching graph* of [20].

6.2. Construction of Hurwitz graphs for $r = 1$. Let $f : C \rightarrow \mathbb{P}^1$ be a simple Hurwitz cover of genus g and degree d with labeled profile (μ_1, \dots, μ_n) over ∞ , unramified over $0 \in \mathbb{P}^1$, and simply ramified over $B = \{\xi^1, \dots, \xi^s\} \subset \mathbb{P}^1$, where $\xi = \exp(2\pi i/s)$ and $s = 2g - 2 + d + n$. We denote by $R = \{p_1, \dots, p_s\} \subset C$ the labeled simple ramification points of f , that is bijectively mapped to B by $f : R \rightarrow B$. We choose a labeling of R so that $f(p_\alpha) = \xi^\alpha$ for every $\alpha = 1, \dots, s$.

On \mathbb{P}^1 , plot B and connect each element $\xi^\alpha \in B$ with 0 by a straight line segment. We also connect 0 and ∞ by a straight line $z = t \exp(\pi i/s)$, $0 \leq t \leq \infty$. Let $*$ denote the configuration of the s line segments. The inverse image $f^{-1}(*)$ is a cell graph on C , for which $f^{-1}(0)$ forms the set of vertices. We remove all inverse images $f^{-1}(\overline{0\xi^\alpha})$ of the line segment $\overline{0\xi^\alpha}$ from this graph, except for the ones that end at one of the points $p_\alpha \in R$. Since p_α is a simple ramification point of f , the line segment ending at p_α extends to another vertex, i.e., another point in $f^{-1}(0)$. We denote by γ^\vee the graph after this removal of line segments. We define the edges of the graph to be the connected line segments at p_α for some α . We use p_α as the label of the edge. The graph γ^\vee has d vertices, s edges, and n faces.

An inverse image of the line $\overline{0\infty}$ is a ray starting at a vertex of the graph γ^\vee and ending up with one of the points in $f^{-1}(\infty)$, which is the center of a face. We place a dot on this line near at each vertex. The edges of γ^\vee incident to a vertex are cyclically ordered counter-clockwise, following the natural cyclic order of B . Let p_α be an edge incident to a vertex, and p_β the next one at the same vertex according to the cyclic order. We denote by $d_{\alpha\beta}$ the number of dots in the span of two edges p_α and p_β , which is 0 if $\alpha < \beta$, and 1 if $\beta < \alpha$. Now we consider the dual graph γ of γ^\vee . It has n vertices, d faces, and s edges still labeled by $\{p_1, \dots, p_s\}$. At the angled corner between the two adjacent edges labeled by p_α and p_β in this order according to the cyclic order, we place $d_{\alpha\beta}$ dots. The data (γ, D) consisting of the cell graph γ and the dot configuration D is the Hurwitz graph corresponding to the simple Hurwitz cover $f : C \rightarrow \mathbb{P}^1$ for $r = 1$.

It is obvious that what we obtain is an $r = 1$ Hurwitz graph, except for the condition (5) of the configuration D , which requires an explanation. The dual graph γ^\vee for $r = 1$ is the *branching graph* of [20]. Since $|B| = s$ is the number of simple ramification points, which is also the number of edges of γ^\vee , the branching graph cannot have any loops. This is because two distinct powers of ξ in the range of $1, \dots, s$ cannot be the same. This fact reflects in the condition that γ has no edge that bounds the same face twice. This explains the condition (5) for $r = 1$.

Remark 6.3. If we consider the case $r = 1, g = 0$ and $n = 1$, then $s = d - 1$. Hence the graph γ^\vee is a connected tree consisting of d nodes (vertices) and $d - 1$ labeled edges. Except for $d = 1, 2$, every vertex is uniquely labeled by incident edges. The tree counting of Introduction is relevant to Hurwitz numbers in this way.

6.3. Construction of r -Hurwitz graphs for $r > 1$. This time we consider an orbifold Hurwitz cover $f : C \rightarrow \mathbb{P}^1[r]$ of genus g and degree $d = rm$ with labeled profile (μ_1, \dots, μ_n) over ∞ , m isomorphic stacky points over $[0/(\mathbb{Z}/(r))] \in \mathbb{P}^1[r]$, and simply ramified over $B = \{\xi^1, \dots, \xi^s\} \subset \mathbb{P}^1[r]$, where $s = 2g - 2 + m + n$. By $R = \{p_1, \dots, p_s\} \subset C$ we indicate the labeled simple ramification points of f , that is again bijectively mapped to B by $f : R \rightarrow B$. We choose the same labeling of R so that $f(p_\alpha) = \xi^\alpha$ for every $\alpha = 1, \dots, s$.

On $\mathbb{P}^1[r]$, plot B and connect each element $\xi^\alpha \in B$ with the stacky point at 0 by a straight line segment. We also connect 0 and ∞ by a straight line $z = t \exp(\pi i/s)$, $0 \leq t \leq \infty$, as before. Let $*$ denote the configuration of the s line segments. The inverse image $f^{-1}(*)$ is

a cell graph on C , for which $f^{-1}(0)$ forms the set of vertices. We remove all inverse images $f^{-1}(\overline{0\xi^\alpha})$ of the line segment $\overline{0\xi^\alpha}$ from this graph, except for the ones that end at one of the points $p_\alpha \in R$. We denote by γ^\vee the graph after this removal of line segments. We define the edges of the graph to be the connected line segments at p_α for some α . We use p_α as the label of the edge. The graph γ^\vee has m vertices, s edges.

The inverse image of the line $\overline{0\infty}$ form a set of r rays at each vertex of the graph γ^\vee , connecting m vertices and n centers $f^{-1}(\infty)$ of faces. We place a dot on each line near at each vertex. These dots are cyclically ordered according to the orientation of C , which we choose to be counter-clock wise. The edges of γ^\vee incident to a vertex are also cyclically ordered in the same way. Let p_α be an edge incident to this vertex, and p_β the next one according to the cyclic order. We denote by $d_{\alpha\beta}$ the number of dots in the span of two edges p_α and p_β . Let γ denote the dual graph of γ^\vee . It now has n vertices, m faces, and s edges still labeled by $\{p_1, \dots, p_s\}$. At the angled corner between the two adjacent edges labeled by p_α and p_β in this order according to the cyclic order, we place $d_{\alpha\beta}$ dots, again cyclically ordered as on γ^\vee . The data (γ, D) consisting of the cell graph γ and the dot configuration D is the r -Hurwitz graph corresponding to the orbifold Hurwitz cover $f : C \rightarrow \mathbb{P}^1[r]$.

We note that γ^\vee can have loops, unlike the case of $r = 1$. Let us place γ^\vee locally on an oriented plane around a vertex. The plane is locally separated into r sectors by the r rays $f^{-1}(\overline{0\infty})$ at this vertex. There are s half-edges coming out of the vertex at each of these r sectors. A half-edge corresponding to ξ^α cannot be connected to another half-edge corresponding to ξ^β in the same sector, by the same reason for the case of $r = 1$. But it can be connected to another half-edge of a different sector corresponding again to the same ξ^α . In this case, within the loop there are some dots, representing the rays of $f^{-1}(\overline{0\infty})$ in between these half-edges. The total number of dots in the loop cannot be r , because then the half-edges being connected are in the same sector. Thus the condition (5) is satisfied.

6.4. An example. Theorem 6.6 below shows that

$$\mathcal{H}_{0,2}^2(3,1) = \frac{9}{2}.$$

This is the weighted count of the number of 2-Hurwitz graphs of type $(g, n, d) = (0, 2, 4)$ with an ordered partition $4 = 3 + 1$.

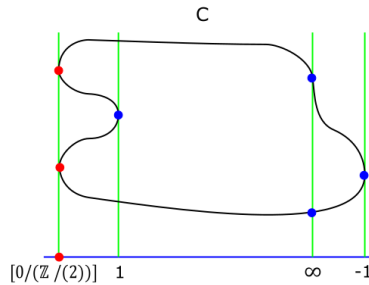


FIGURE 6.2. Hurwitz covers counted in $\mathcal{H}_{0,2}^2(3,1)$ have two orbifolds points, two simple ramification points, and one ramification point of degree 3.

In terms of formulas, the 2-Hurwitz cover corresponding to the graph on the left of Figure 6.3 is given by

$$f(x) = \frac{(x-1)^2(x+1)^2}{x}.$$

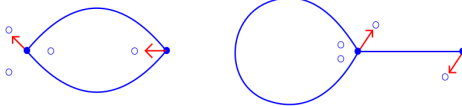


FIGURE 6.3. There are two 2-Hurwitz graphs. The number of graphs is $3/2$ for the graph on the left counting the automorphism, and 3 for the one on the right. The total is thus $9/2$.

To make the simple ramification points sit on ± 1 , we need to divide $f(x)$ by $f(i/\sqrt{3})$, where $x = \pm 1/\sqrt{3}$ are the simple ramification points. The 2-Hurwitz cover corresponding to the graph on the right of Figure 6.3 is given by

$$f(x) = \frac{(x-1)^2(x+1)^2}{x-a},$$

where a is a real number satisfying $|a| > \sqrt{3}/2$. The real parameter a changes the topological type of the 2-Hurwitz cover. For $-\frac{\sqrt{3}}{2} < a < \frac{\sqrt{3}}{2}$, the graph is the same as on the left, and for $|a| > \frac{\sqrt{3}}{2}$, the graph becomes the one on the right.

6.5. The edge-contraction formulas.

Definition 6.4 (Edge-contraction operations). The edge-contraction operations (ECOs) on an arrowed r -Hurwitz graph (γ, \vec{D}) are the following procedures. Choose an edge E of the cell graph γ .

- **ECO 1:** We consider the case that E is an edge connecting two distinct vertices Vertex i and Vertex j . We can assume $i < j$, which induces a direction $i \xrightarrow{E} j$ on E . Let us denote by F_+ and F_- the faces bounded by E , where F_+ is on the left side of E with respect to the direction. We now contract E , with the following additional operations:
 - (1) Remove the original arrows at Vertices i and j .
 - (2) Put the dots on F_{\pm} clustered at Vertices i and j together, keeping the cyclic order of the dots on each of F_{\pm} .
 - (3) Place a new arrow to the largest dot on the corner at Vertex i of Face F_+ with respect to the cyclic order.
 - (4) If there are no dots on this particular corner, then place an arrow to the first dot we encounter according to the counter-clock wise rotation from E and centered at Vertex i .

The new arrow at the joined vertex allows us to recover the original graph from the new one.

- **ECO 2:** This time E is a loop incident to Vertex i twice. We contract E and separate the vertex into two new ones, as in ECA 3 of Definition 4.4. The additional operations are:
 - (1) The contraction of a loop does not change the number of faces. Separate the dots clustered at Vertex i according to the original configuration.
 - (2) Look at the new vertex to which the original arrow is placed. We keep the same name i to this vertex. The other vertex is named i' .
 - (3) Place a new arrow to the dot on the corner at the new Vertex i that was the largest in the original corner with respect to the cyclic order.

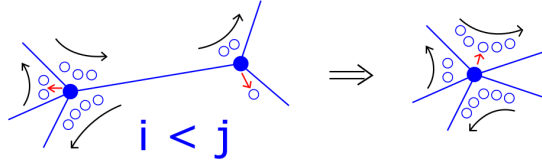


FIGURE 6.4. After contracting the edge, a new arrow is placed on the dot that is the largest (according to the cyclic order) around Vertex i in the original graph, and on the face incident to E which is on the left of E with respect to the direction $i \rightarrow j$. The new arrow tells us where the break is made in the original graph. If there are no dots on this particular face, then we go around Vertex i counter-clock wise and find the first dot in the original graph. We place an arrow to this dot in the new graph after contracting E . Here again the purpose is to identify which of the μ_i dots come from the original Vertex i

- (4) If there are no dots on this particular corner, then place an arrow to the first dot we encounter according to the counter-clock wise rotation from E and centered at Vertex i on the side of the old arrow.
- (5) We do the same operation for the new Vertex i' , and put a new arrow to a dot.
- (6) Now remove the original arrow.

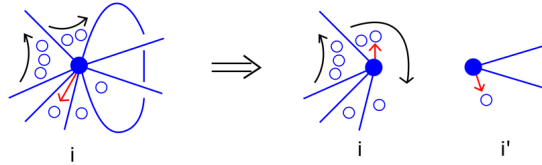


FIGURE 6.5. New arrows are placed so that the original graph can be recovered from the new one

Although cumbersome, it is easy to show that

Lemma 6.5. *The edge-contraction operations preserve the set of r -Hurwitz graphs.*

An application of the edge-contraction operations is the following counting recursion formula.

Theorem 6.6 (Edge-Contraction Formula). *The number of arrowed Hurwitz graphs satisfy the following edge-contraction formula.*

$$\begin{aligned}
& \left(2g - 2 + \frac{d}{r} + n\right) \mathcal{H}_{g,n}^r(\mu_1, \dots, \mu_n) \\
&= \sum_{i < j} \mu_i \mu_j \mathcal{H}_{g,n-1}^r(\mu_1, \dots, \mu_{i-1}, \mu_i + \mu_j, \mu_{i+1}, \dots, \widehat{\mu_j}, \dots, \mu_n) \\
(6.4) \quad &+ \frac{1}{2} \sum_{i=1}^n \mu_i \sum_{\substack{\alpha + \beta = \mu_i \\ \alpha, \beta \geq 1}} \left[\mathcal{H}_{g-1,n+1}^r(\alpha, \beta, \mu_1, \dots, \widehat{\mu_i}, \dots, \mu_n) \right. \\
&\quad \left. + \sum_{\substack{g_1 + g_2 = g \\ I \sqcup J = \{1, \dots, \widehat{i}, \dots, n\}}} \mathcal{H}_{g_1, |I|+1}^r(\alpha, \mu_I) \mathcal{H}_{g_2, |J|+1}^r(\beta, \mu_J) \right].
\end{aligned}$$

Here, $\widehat{}$ indicates the omission of the index, and $\mu_I = (\mu_i)_{i \in I}$ for any subset $I \subset \{1, 2, \dots, n\}$.

Remark 6.7. The edge-contraction formula (ECF) is a recursion with respect to the number of edges

$$s = 2g - 2 + \frac{\mu_1 + \dots + \mu_n}{r} + n.$$

Therefore, it calculates all values of $\mathcal{H}_{g,n}^r(\mu_1, \dots, \mu_n)$ from the base case $\mathcal{H}_{0,1}^r(r)$. However, it does not determine the initial value itself, since $s = 0$. We also note that the recursion is not for $\mathcal{H}_{g,n}^r$ as a function in n integer variables.

Proof. The counting is done by applying the edge-contraction operations. The left-hand side of (6.4) shows the choice of an edge, say E , out of $s = 2g - 2 + \frac{d}{r} + n$ edges. The first line of the right-hand side corresponds to the case that the chosen edge E connects Vertex i and Vertex j . We assume $i < j$, and apply ECO 1. The factor $\mu_i \mu_j$ indicates the removal of two arrows at these vertices (Figure 6.4).

When the edge E we have chosen is a loop incident to Vertex i twice, then we apply ECO 2. The factor μ_i is the removal of the original arrow (Figure 6.5). The second and third lines on the right-hand side correspond whether E is a handle-cutting loop, or a separation loop. The factor $\frac{1}{2}$ is there because of the symmetry between α and β of the partition of μ_i . This complete the proof. \square

Theorem 6.8 (Graph enumeration and orbifold Hurwitz numbers). *The graph enumeration and counting orbifold Hurwitz number are related by the following formula:*

$$(6.5) \quad \mathcal{H}_{g,n}^r(\mu_1, \dots, \mu_n) = \mu_1 \mu_2 \cdots \mu_n H_{g,n}^r(\mu_1, \dots, \mu_n).$$

Proof. The simplest orbifold Hurwitz number is $H_{0,1}^r(r)$, which counts double Hurwitz numbers with the same profile (r) at both $0 \in \mathbb{P}^1$ and $\infty \in \mathbb{P}^1$. There is only one such map $f : \mathbb{P}^1 \rightarrow \mathbb{P}^1$, which is given by $f(x) = x^r$. Since the map has automorphism $\mathbb{Z}/(r)$, we have $H_{0,1}^r(r) = 1/r$. Thus (6.5) holds for the base case.

We notice that (6.4) is exactly the same as the cut-and-join equation of [3, Theorem 2.2], after modifying the orbifold Hurwitz numbers by multiplying $\mu_1 \cdots \mu_n$. Since the initial value is the same, and the formulas are recursion based on $s = 2g - 2 + \frac{d}{r} + n$, (6.5) holds by induction. This completes the proof. \square

7. CONSTRUCTION OF THE MIRROR SPECTRAL CURVES FOR ORBIFOLD HURWITZ NUMBERS

In the earlier work on simple and orbifold Hurwitz numbers in connection to the topological recursion [3, 4, 6, 12, 19], the spectral curves are determined by the infinite framing limit of the mirror curves to toric Calabi-Yau (orbi-)threefolds. The other ingredients of the topological recursion, the differential forms $W_{0,1}$ and $W_{0,2}$, are calculated by the Laplace transform of the $(g, n) = (0, 1)$ and $(0, 2)$ cases of the ELSV [11] and JPT [14] formulas. Certainly the logic is clear, but why these choices are the right ones is not well explained.

In this section, we show that the edge-contraction operations themselves determine all the mirror ingredients, i.e., the spectral curve, $W_{0,1}$, and $W_{0,2}$. The structure of the story is the following. The edge-contraction formula (6.4) is an equation among different values of (g, n) . When restricted to $(g, n) = (0, 1)$, it produces an equation on $\mathcal{H}_{0,1}^r(d)$ as a function in one integer variable. The generating function of $\mathcal{H}_{g,n}^r(\mu_1, \dots, \mu_n)$ is reasonably complicated, but it can be expressed rather nicely in terms of the generating function of the $(0, 1)$ -values $\mathcal{H}_{0,1}^r(d)$, which is essentially the spectral curve of the theory. The edge-contraction formula (6.4) itself has the Laplace transform that can be calculated in the spectral curve coordinate. Since (6.4) contains (g, n) on each side of the equation, to make it a genuine recursion formula for functions with respect to $2g - 2 + n$ in the stable range, we need to calculate the generating functions of $\mathcal{H}_{0,1}^r(d)$ and $\mathcal{H}_{0,2}^r(\mu_1, \mu_2)$, and make the rest of (6.4) free of unstable terms. The result is the topological recursion of [3, 12].

Let us now start with the restricted (6.4) on $(0, 1)$ invariants:

$$(7.1) \quad \left(\frac{d}{r} - 1 \right) \mathcal{H}_{0,1}^r(d) = \frac{1}{2} d \sum_{\substack{\alpha+\beta=d \\ \alpha, \beta \geq 1}} \mathcal{H}_{0,1}^r(\alpha) \mathcal{H}_{0,1}^r(\beta).$$

At this stage, we introduce a generating function

$$(7.2) \quad y = y(x) = \sum_{d=1}^{\infty} \mathcal{H}_{0,1}^r(d) x^d.$$

In terms of this generating function, (7.1) is a differential equation

$$(7.3) \quad \left(x^{r+1} \circ \frac{d}{dx} \circ \frac{1}{x^r} \right) y = \frac{1}{2} r x \frac{d}{dx} y^2,$$

or simply

$$\frac{y'}{y} - r y' = \frac{r}{x}.$$

Its unique solution is

$$Cx^r = y e^{-ry}$$

with a constant of integration C . As we noted in the previous section, the recursion (6.4) does not determine the initial value $\mathcal{H}_{0,1}^r(d)$. For our graph enumeration problem, the values are

$$(7.4) \quad \mathcal{H}_{0,1}^r(d) = \begin{cases} 0 & 1 \leq d < r; \\ 1 & d = r, \end{cases}$$

which determine $C = 1$. Thus we find

$$(7.5) \quad x^r = y e^{-ry},$$

which is the r -Lambert curve of [3]. This is indeed the spectral curve for the orbifold Hurwitz numbers.

Remark 7.1. We note that $r\mathcal{H}_{0,1}^r(rm)$ satisfies the same recursion equation (7.1) for $r = 1$, with a different initial value. Thus essentially orbifold Hurwitz numbers are determined by the usual simple Hurwitz numbers.

Remark 7.2. If we define $T_d = (d-1)! \mathcal{H}_{0,1}^{r=1}(d)$, then (7.1) for $r = 1$ is equivalent to (1.2). This is the reason we consider the tree recursion as the spectral curve for simple and orbifold Hurwitz numbers.

For the purpose of performing analysis on the spectral curve (7.5), let us introduce a global coordinate z on the r -Lambert curve, which is an analytic curve of genus 0:

$$(7.6) \quad \begin{cases} x = x(z) := ze^{-z^r} \\ y = y(z) := z^r. \end{cases}$$

We denote by $\Sigma \subset \mathbb{C}^2$ this parametric curve. Let us introduce the generating functions of general $\mathcal{H}_{g,n}^r$, which are called *free energies*:

$$(7.7) \quad F_{g,n}(x_1, \dots, x_n) := \sum_{\mu_1, \dots, \mu_n \geq 1} \frac{1}{\mu_1 \cdots \mu_n} \mathcal{H}_{g,n}^r(\mu_1, \dots, \mu_n) \prod_{i=1}^n x_i^{\mu_i}.$$

We also define the exterior derivative

$$(7.8) \quad W_{g,n}(x_1, \dots, x_n) := d_1 \cdots d_n F_{g,n}(x_1, \dots, x_n),$$

which is a symmetric n -linear differential form. By definition, we have

$$(7.9) \quad y = y(x) = x \frac{d}{dx} F_{0,1}(x).$$

The topological recursion requires the spectral curve, $W_{0,1}$, and $W_{0,2}$. From (7.8) and (7.9), we have

$$(7.10) \quad W_{0,1}(x) = y \frac{dx}{x} = y d \log(x).$$

Remark 7.3. For many examples of topological recursion such as ones considered in [10], we often define $W_{0,1} = y dx$, which is a holomorphic 1-form on the spectral curve. For Hurwitz theory, due to (7.9), it is more natural to use (7.10).

As a differential equation, we can solve (7.9) in a closed formula on the spectral curve Σ of (7.6). Indeed, the role of the spectral curve is that the free energies, i.e., $F_{g,n}$'s, are actually analytic functions defined on Σ^n . Although we define $F_{g,n}$'s as a formal power series in (x_1, \dots, x_n) as generating functions, they are analytic, and the domain of analyticity, or the classical sense of *Riemann surface*, is the spectral curve Σ . The coordinate change (7.6) gives us

$$(7.11) \quad x \frac{d}{dx} = \frac{z}{1 - rz^r} \frac{d}{dz},$$

hence (7.9) is equivalent to

$$z^{r-1} (1 - rz^r) = \frac{d}{dz} F_{0,1}(x(z)).$$

Since $z = 0 \implies x = 0 \implies F_{0,1}(x) = 0$, we find

$$(7.12) \quad F_{0,1}(x(z)) = \frac{1}{r} z^r - \frac{1}{2} z^{2r}.$$

The calculation of $F_{0,2}$ is done similarly, by restricting (6.4) to the $(g, n) = (0, 1)$ and $(0, 2)$ terms. Assuming that $\mu_1 + \mu_n = mr$, we have

$$(7.13) \quad \begin{aligned} & \left(\frac{d}{r} - 1 \right) \mathcal{H}_{0,2}^r(\mu_1, \mu_2) \\ &= \mu_1 \mu_2 \mathcal{H}_{0,1}^r(\mu_1 + \mu_2) + \mu_1 \sum_{\substack{\alpha + \beta = \mu_1 \\ \alpha, \beta > 0}} \mathcal{H}_{0,1}^r(\alpha) \mathcal{H}_{0,2}^r(\beta, \mu_2) + \mu_2 \sum_{\substack{\alpha + \beta = \mu_2 \\ \alpha, \beta > 0}} \mathcal{H}_{0,1}^r(\alpha) \mathcal{H}_{0,2}^r(\mu_1, \beta). \end{aligned}$$

As a special case of [3, Lemma 4.1], this equation translates into a differential equation for $F_{0,2}$:

$$(7.14) \quad \begin{aligned} & \frac{1}{r} \left(x_1 \frac{\partial}{\partial x_1} + x_2 \frac{\partial}{\partial x_2} \right) F_{0,2}(x_1, x_2) \\ &= \frac{1}{x_1 - x_2} \left(x_1^2 \frac{\partial}{\partial x_1} F_{0,1}(x_1) - x_2^2 \frac{\partial}{\partial x_2} F_{0,1}(x_2) \right) - \left(x_1 \frac{\partial}{\partial x_1} F_{0,1}(x_1) + x_2 \frac{\partial}{\partial x_2} F_{0,1}(x_2) \right) \\ &+ \left(x_1 \frac{\partial}{\partial x_1} F_{0,1}(x_1) \right) \left(x_1 \frac{\partial}{\partial x_1} F_{0,2}(x_1, x_2) \right) + \left(x_2 \frac{\partial}{\partial x_2} F_{0,1}(x_2) \right) \left(x_2 \frac{\partial}{\partial x_2} F_{0,2}(x_1, x_2) \right). \end{aligned}$$

Denoting by $x_i = x(z_i)$ and using (7.11), (7.14) becomes simply

$$(7.15) \quad \frac{1}{r} \left(z_1 \frac{\partial}{\partial z_1} + z_2 \frac{\partial}{\partial z_2} \right) F_{0,2}(x(z_1), x(z_2)) = \frac{x_1 z_1^r - x_2 z_2^r}{x_1 - x_2} - (z_1^r + z_2^r)$$

on the spectral curve Σ . This is a linear partial differential equation of the first order with analytic coefficients in the neighborhood of $(0, 0) \in \mathbb{C}^2$, hence by the Cauchy-Kovalevskaya theorem, it has the unique analytic solution around the origin of \mathbb{C}^2 for any Cauchy problem. Since the only analytic solution to the homogeneous equation

$$\left(z_1 \frac{\partial}{\partial z_1} + z_2 \frac{\partial}{\partial z_2} \right) f(z_1, z_2) = 0$$

is a constant, the initial condition $F_{0,2}(0, x_2) = F_{0,2}(x_1, 0) = 0$ determines the unique solution of (7.15).

Proposition 7.4. *We have a closed formula for $F_{0,2}$ in the z -coordinates:*

$$(7.16) \quad F_{0,2}(x(z_1), x(z_2)) = \log \frac{z_1 - z_2}{x(z_1) - x(z_2)} - (z_1^r + z_2^r).$$

Proof. We first note that $\log \frac{z_1 - z_2}{x(z_1) - x(z_2)}$ is holomorphic around $(0, 0) \in \mathbb{C}^2$. (7.16) being a solution to (7.15) is a straightforward calculation that can be verified as follows:

$$\begin{aligned} & \left(z_1 \frac{\partial}{\partial z_1} + z_2 \frac{\partial}{\partial z_2} \right) \log \frac{z_1 - z_2}{x(z_1) - x(z_2)} \\ &= \frac{z_1 - z_2}{z_1 - z_2} - \frac{z_1 e^{-z_1^r} (1 - r z_1^r) - z_2 e^{-z_2^r} (1 - r z_2^r)}{x_1 - x_2} \\ &= 1 - \frac{x_1 - x_2}{x_1 - x_2} + r \frac{x_1 z_1^r - x_2 z_2^r}{x_1 - x_2} = r \frac{x_1 z_1^r - x_2 z_2^r}{x_1 - x_2}. \end{aligned}$$

Since $F_{0,2}(x(0), x(z_2)) = \log e^{z_2^r} - z_2^r = 0$, (7.16) is the desired unique solution. \square

In [3], the functions (7.12) and (7.16) are derived by directly computing the Laplace transform of the JPT formulas [14]

$$(7.17) \quad H_{0,1}^r(d) = \frac{d^{\lfloor \frac{d}{r} \rfloor - 2}}{\lfloor \frac{d}{r} \rfloor!},$$

$$H_{0,2}^r(\mu_1, \mu_2) = \begin{cases} r^{\langle \frac{\mu_1}{r} \rangle + \langle \frac{\mu_2}{r} \rangle} \frac{1}{\mu_1 + \mu_2} \frac{\mu_1^{\lfloor \frac{\mu_1}{r} \rfloor} \mu_2^{\lfloor \frac{\mu_2}{r} \rfloor}}{\lfloor \frac{\mu_1}{r} \rfloor! \lfloor \frac{\mu_2}{r} \rfloor!} & \mu_1 + \mu_2 \equiv 0 \pmod{r} \\ 0 & \text{otherwise.} \end{cases}$$

Here, $q = \lfloor q \rfloor + \langle q \rangle$ gives the decomposition of a rational number $q \in \mathbb{Q}$ into its floor and the fractional part. We have thus recovered (7.17) from the edge-contraction formula alone, which are the (0, 1) and (0, 2) cases of the ELSV formula for the orbifold Hurwitz numbers.

Acknowledgement. The authors are grateful to the American Institute of Mathematics in California, the Banff International Research Station, the Institute for Mathematical Sciences at the National University of Singapore, Kobe University, the Lorentz Center for Mathematical Sciences, Leiden, and Max-Planck-Institut für Mathematik in Bonn, for their hospitality and financial support during the authors' stay for collaboration. They also thank Ruian Chen, Maxim Kontsevich and Shintaro Yanagida for valuable discussions. O.D. thanks the Perimeter Institute for Theoretical Physics, and M.M. thanks the Hong Kong University of Science and Technology and the Simons Center for Geometry and Physics, for financial support and hospitality. The research of O.D. has been supported by GRK 1463 *Analysis, Geometry, and String Theory* at the Leibniz Universität Hannover. The research of M.M. has been supported by NSF grants DMS-1104734, DMS-1309298, and NSF-RNMS: Geometric Structures And Representation Varieties (GEAR Network, DMS-1107452, 1107263, 1107367).

REFERENCES

- [1] L. Abrams, *Two-dimensional topological quantum field theories and Frobenius algebras*, Journal of Knot Theory and Ramifications **5**, 335–352 (2000).
- [2] M.F. Atiyah, *Topological quantum field theory*, [arXiv:hep-th/0312085], Publications Mathématiques de l'I.H.É.S., **68**, 175–186 (1988).
- [3] V. Bouchard, D. Hernández Serrano, X. Liu, and M. Mulase, *Mirror symmetry for orbifold Hurwitz numbers*, arXiv:1301.4871 [math.AG] (2013).
- [4] V. Bouchard and M. Mariño, *Hurwitz numbers, matrix models and enumerative geometry*, Proc. Symposia Pure Math. **78**, 263–283 (2008).
- [5] R. Chen, *Topological quantum field theory from the viewpoint of cellular graphs*, Senior Thesis, University of California, Davis (2015).
- [6] N. Do, O. Leigh, and P. Norbury, *Orbifold Hurwitz numbers and Eynard-Orantin invariants*, arXiv:1212.6850 (2012).
- [7] O. Dumitrescu, D. Hernández Serrano, and M. Mulase, *TQFT-valued topological recursion*, in preparation.
- [8] O. Dumitrescu and M. Mulase, *Quantum curves for Hitchin fibrations and the Eynard-Orantin theory*, Lett. Math. Phys. **104**, 635–671 (2014).
- [9] O. Dumitrescu and M. Mulase, *Quantization of spectral curves for meromorphic Higgs bundles through topological recursion*, arXiv:1411.1023 (2014).
- [10] O. Dumitrescu, M. Mulase, A. Sorkin and B. Safnuk, *The spectral curve of the Eynard-Orantin recursion via the Laplace transform*, in “Algebraic and Geometric Aspects of Integrable Systems and Random Matrices,” Dzhumayev, Maruno and Pierce, Eds. Contemporary Mathematics **593**, 263–315 (2013).
- [11] T. Ekedahl, S. Lando, M. Shapiro, A. Vainshtein, *Hurwitz numbers and intersections on moduli spaces of curves*, Invent. Math. **146**, 297–327 (2001) [arXiv:math/0004096].
- [12] B. Eynard, M. Mulase and B. Safnuk, *The Laplace transform of the cut-and-join equation and the Bouchard-Mariño conjecture on Hurwitz numbers*, Publications of the Research Institute for Mathematical Sciences **47**, 629–670 (2011).
- [13] B. Eynard and N. Orantin, *Invariants of algebraic curves and topological expansion*, Communications in Number Theory and Physics **1**, 347–452 (2007).

- [14] P. Johnson, R. Pandharipande, and H.H. Tseng, *Abelian Hurwitz-Hodge integrals*, Michigan Math. J. **60**, 171–198 (2011) [arXiv:0803.0499].
- [15] J. Kock, *Frobenius algebras and 2D topological quantum field theories*, Cambridge University Press (2003).
- [16] M. Kontsevich and Yuri Manin, *Gromov-Witten classes, quantum cohomology, and enumerative geometry*, Communications in Mathematical Physics **164**, 525–562 (1994).
- [17] M. Mulase and M. Penkava, *Ribbon graphs, quadratic differentials on Riemann surfaces, and algebraic curves defined over $\overline{\mathbb{Q}}$* , The Asian Journal of Mathematics **2** (4), 875–920 (1998).
- [18] M. Mulase and P. Sułkowski, *Spectral curves and the Schrödinger equations for the Eynard-Orantin recursion*, arXiv:1210.3006 (2012).
- [19] M. Mulase and N. Zhang, *Polynomial recursion formula for linear Hodge integrals*, Communications in Number Theory and Physics **4**, 267–294 (2010).
- [20] A. Okounkov and R. Pandharipande, *Gromov-Witten theory, Hurwitz numbers, and matrix models, I*, Proc. Symposia Pure Math. **80**, 325–414 (2009).
- [21] G. Segal, *Geometric aspect of quantum field theory*, Proceedings of the International Congress of Mathematicians, Kyoto, Japan 1990, 1387–1396 (1991).
- [22] C. Teleman, *The structure of 2D semi-simple field theories*, Inventiones Mathematicae **188**, 525–588 (2012).
- [23] T.R.S. Walsh and A.B. Lehman, *Counting rooted maps by genus. I*, Journal of Combinatorial Theory **B-13**, 192–218 (1972).

O. DUMITRESCU, INSTITUT FÜR ALGEBRAISCHE GEOMETRIE, FAKULTÄT FÜR MATHEMATIK UND PHYSIK, LEIBNIZ UNIVERSITÄT HANNOVER, WELFENGARTEN 1, 30167 HANNOVER,

E-mail address: dumitrescu@math.uni-hannover.de

MAX-PLANCK-INSTITUT FÜR MATHEMATIK, BONN, GERMANY

M. MULASE, DEPARTMENT OF MATHEMATICS, UNIVERSITY OF CALIFORNIA, DAVIS, CA 95616–8633, U.S.A.,

E-mail address: mulase@math.ucdavis.edu

KAVALI INSTITUTE FOR PHYSICS AND MATHEMATICS OF THE UNIVERSE, THE UNIVERSITY OF TOKYO, KASHIWA, JAPAN